UCRL 8733

UNIVERSITY OF CALIFORNIA

Ernest O. Lawrence

Radiation Laboratory

COALESCENCE AND DISPERSION RATES IN AGITATED LIQUID-LIQUID SYSTEMS

BERKELEY, CALIFORNIA

DISCLAIMER

This document was prepared as an account of work sponsored by the United States Government. While this document is believed to contain correct information, neither the United States Government nor any agency thereof, nor the Regents of the University of California, nor any of their employees, makes any warranty, express or implied, or assumes any legal responsibility for the accuracy, completeness, or usefulness of any information, apparatus, product, or process disclosed, or represents that its use would not infringe privately owned rights. Reference herein to any specific commercial product, process, or service by its trade name, trademark, manufacturer, or otherwise, does not necessarily constitute or imply its endorsement, recommendation, or favoring by the United States Government or any agency thereof, or the Regents of the University of California. The views and opinions of authors expressed herein do not necessarily state or reflect those of the United States Government or any agency thereof or the Regents of the University of California.

UCRL-8733
Chemistry Distribution
TID-4500 (15th Ed.)

UNIVERSITY OF CALIFORNIA

Lawrence Radiation Laboratory
Berkeley, California

Contract No. W-7405-eng-48

COALESCENCE AND DISPERSON RATES IN AGITATED LIQUID-LIQUID SYSTEMS

James Hidde Vanderveen

M. S. Thesis

December 1960

Printed in USA. Price $1.25. Available from the
Office of Technical Services
U. S. Department of Commerce
Washington 25, D.C.

COALESCENCE AND DISPERSON RATES IN AGITATED LIQUID-LIQUID SYSTEMS

Contents

Abstract 3

Introduction 4

Coalescence Study 8

- Apparatus Assembly 8
- Light-Transmission Measurements 12

Operating Procedure 18

- Sources of Error 19

Results and Discussion

- Variation of Drop Diameter with Probe Position . . . 20
- Correlation 26
- Comparison with Rodger's Results 38

Dispersion Studies

- Measurements 43
- Results 43

Conclusions 46

Notation 47

Literature Cited 49

Appendix

- Numerical Data 50
- Photoelectric-Probe Calibration Curves 54

COALESCENCE AND DISPERSON RATES IN AGITATED LIQUID-LIQUID SYSTEMS

James Hidde Vanderveen

Department of Chemical Engineering and Lawrence Radiation Laboratory
University of California, Berkeley, California

December 1960

ABSTRACT

In previous work at this Laboratory, the drop diameter at the impeller tip (also referred to as the minimum drop diameter) of a mixture of two immiscible liquids in a stirred tank has been found to be a function of Weber number and of a volume-fraction parameter.

This study has aimed at determining the variables affecting the coalescence of droplets after they leave the impeller tip. The resulting correlation shows that the mean drop diameter at any position in a stirred tank can be expressed as the sum of the equilibrium drop diameter and an incremental coalescence term which is a function of viscosities, densities, volume fraction, and Weber and Reynolds numbers.

The rate of dispersion of a dye soluble only in the dispersed phase of an agitated liquid-liquid mixture has also been found to be a function of Weber and Reynolds numbers.

INTRODUCTION

Mixing of two immiscible liquids is used widely for such operations as solvent extraction, heterogeneous reactions, and emulsification. Investigations in the agitation of such mixtures have usually been concerned with power requirements, effectiveness of mixing, and interfacial area produced per unit volume of fluid. Knowledge of this specific interfacial area is of special interest for operations involving transfer of material from one phase to another.

Clay (3) studied the effect of fluid variables on drop size in a highly turbulent liquid-liquid system. Two different types of experimental apparatus were used. One utilized high-speed flow of the immiscible liquids through a closed pipe circuit; the other, rotation at high speeds of the inner cylinder of a concentric pair. In each case, the range of Reynolds numbers was 50,000-500,000. Drop sizes were determined by taking high-speed photographs of the emulsions.

Langlois and co-workers developed a photoelectric probe to measure the scattering of light by unstable emulsions (6). Calibration of this probe, by high-speed photography and simultaneous photocell readings, yielded a relation between photocell current output and specific interfacial area (or area per unit volume), A:

$$I_0/I = \beta A + 1 \ . \qquad (1)$$

---

*This work was done under the auspices of the U. S. Atomic Energy Commission.

The extinction ratio, I_0/I, depends upon the initial photocell reading, (I_0), of the clear continuous phase, and that of the photocell output (I), under mixing conditions. The slope β of the equation is a function of the ratio (m) of the refractive index of the immiscible liquids.

Vermeulen, Williams, and Langlois (14) developed an empirical correlation for liquid-liquid systems, relating the surface-mean drop diameter to the Weber number. With consistent units, the specific interfacial area was found to be given by the relation:

$$A = 72N^{1.2} L^{0.8} \bar{\rho}^{0.6} \phi/\sigma^{0.6} f_\phi \qquad (2)$$

where, for spherical drops, the mean diameter is $d=6\phi/A$; $\phi(=\phi_d)$ is the volume fraction of dispersed phase; N is the agitator speed, revolutions per unit time; L is the impeller diameter; $\bar{\rho}$ is an effective mean density ($0.6\ \rho_d + 0.4\ \rho_c$) where ρ_d and ρ_c are densities of the dispersed and continuous phases respectively; σ is the interfacial tension; and f_ϕ is a volume-fraction correlation factor given by

$$f_\phi = 0.75 + 2.5\phi \ . \qquad (2a)$$

Fick, Rea, and Vermeulen (4) extended this work by investigating the effect of changing various geometrical factors such as impeller size and tank size. This study agreed with the previous correlation, although with a considerable scatter of points.

Rodger, Trice, and Rushton (9) arrived at a more complex correlation relating interfacial area to the 0.36power of the Weber number with additional contributions from viscosity effects, density differences, and a settling factor determined from a separate settling test on the immiscible system. The experimental conditions in this investigation were dissimilar, in that the photocell readings were taken at different points in the mixing tank (Langlois's and Fick's readings were taken opposite the impeller tip, whereas Rodger's were taken at the bottom); and a somewhat different design of impeller was used.

Hinze (5) has developed a theoretical analysis of droplet breakup which can be used to express d_{max}, the diameter of the largest droplets which will emerge unsplit from a given region of turbulence under equilibrium breakup conditions. In Hinze's treatment, the dynamic pressure forces of turbulent motion are expressed in a Weber number which has a characteristic critical value for breakup:

$$(N_{We})_{crit} = \rho_c \overline{v^2} d_{max}/\sigma = \text{constant} \tag{3}$$

where $\overline{v^2}$ is the average value of the squares of velocity fluctuations over a distance equal to d_{max}. Batchelor (1) has applied the Kolmogoroff energy-distribution law to obtain:

$$\overline{v^2} = 2\,(E\, d_{max})^{2/3}. \tag{4}$$

Here E is the power input per unit mass; hence

$$\overline{v^2} = 2\,(P\, d_{max}/\, V\rho')^{2/3} \tag{5}$$

where $\rho' = \rho_c + (\rho_d - \rho_c)\,\phi$, the volumetric mean density; and V is the volume of the flow field involving maximum turbulence.

Studies in this laboratory have shown that (4)

$$P/\rho' = 20.4\, N^3 L^4 W/g_c \tag{6}$$

where W is the impeller width, and the constant of 20.4 applies to a four-bladed flat paddle under standard baffling. The constant g_c will be unity if P is expressed in mass-length-time units. It is reasonable to assume empirically that V is proportional to the space swept through by the impeller:

$$V = C^{3/2}\, L^2\, W \tag{7}$$

where C is an unknown constant. Hence

$$P/V\rho' = 20.4\, N^3\, L^2/C^{3/2}\ .$$

By applying this theory of Clay's results, Hinze obtained $(N_{We})_{crit}=1.18$. With this value, the theoretical equation becomes

$$d_{max}^{5/3} N^2 L^{4/3} \rho_c/\sigma = 1.18C/2(20.4)^{2/3} = 0.0790 \quad . \tag{8}$$

The correlation of Vermeulen, Langlois, and Williams (14) can be expressed in a similar form. At ϕ approaches 0, f_ϕ in that correlation is 0.75; results to the present investigation suggest that d_0, the surface-mean diameter under equilibrium-breakup conditions, will be further reduced by a factor of 0.88, due to the average coalescence that had occurred in the earlier study. The effective mean density was selected for other theoretical reasons; it can be replaced by ρ_c without loss in accuracy. Hence the experimental correlation becomes

$$d_0^{5/3} N^2 L^{4/3} \rho_c/\sigma = [6(0.75)0.88/72]^{5/3} = 0.080 \quad . \tag{9}$$

This corresponds to Hinze's result, with his apparent $(N_{We})_{crit}$, if $C = 0.080/0.079 \approx 1.0$. It is of interest, that the constant C is essentially unity, as this corroborates the assumption that Batchelor's V is a function of the impeller dimensions rather than of the entire mixing vessel. The similarity between Hinze's result and the correlation of Vermeulen, Williams, and Langlois has also been shown by Calderbank (2) and Webster (15).

COALESCENCE STUDY

This study is an extension of previous work (4), in which it was found that the interfacial area often does not remain constant throughout the tank. This study has been aimed at determining the area at several points in the mixing tank, so as to measure the variation of the specific interfacial area under steady-state conditions. In order to obtain additional knowledge of emulsion behavior, measurements were also made of the rate of dispersion of indicators which were soluble only in the discontinuous phase.

It is found that the use of a relatively small impeller, in a liquid-liquid system having a moderately low interfacial tension, results in a substantial drop-size variation.The drops are smallest opposite the impeller tip, and largest at points near the extreme top and bottom of the mixing tank.

The variables involved in this study are:

a. impeller speed.

b. volume-fraction of dispersed phase (usually 0.10 and 0.40).

c. geometrical location of photoelectric probe; five positions were used, as shown in Fig. 1.

d. physical properties of the two liquids, as listed in Table I.

Apparatus Assembly

The mixing vessel used was a cylindrical stainless steel tank; dimensions were the same as those used by Langlois: height (H) = 8.87 in., diameter (T) = 10.35 in.

Two four-bladed flat-paddle impellers were used; both 5.0 in. in diameter. The impeller usually used had a 1.0-inch width; the other, 2.0 inches. They were centered vertically in all runs.

Figure 2 shows a drawing of the tank as mounted in a steel frame. The ten-inch tank was suspended from, and removable from, its cover. The cover was attached to the frame by means of an integral-suspension ball-bearing unit to which it was welded. A spindle assembly with two

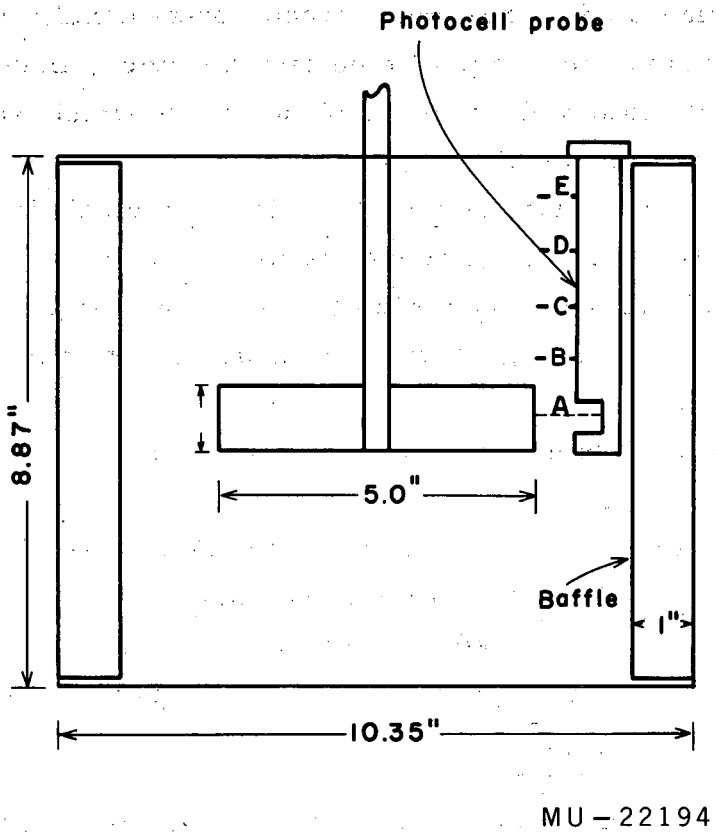

Fig. 1. Side view of mixing tank, showing impeller, probe, and baffles.

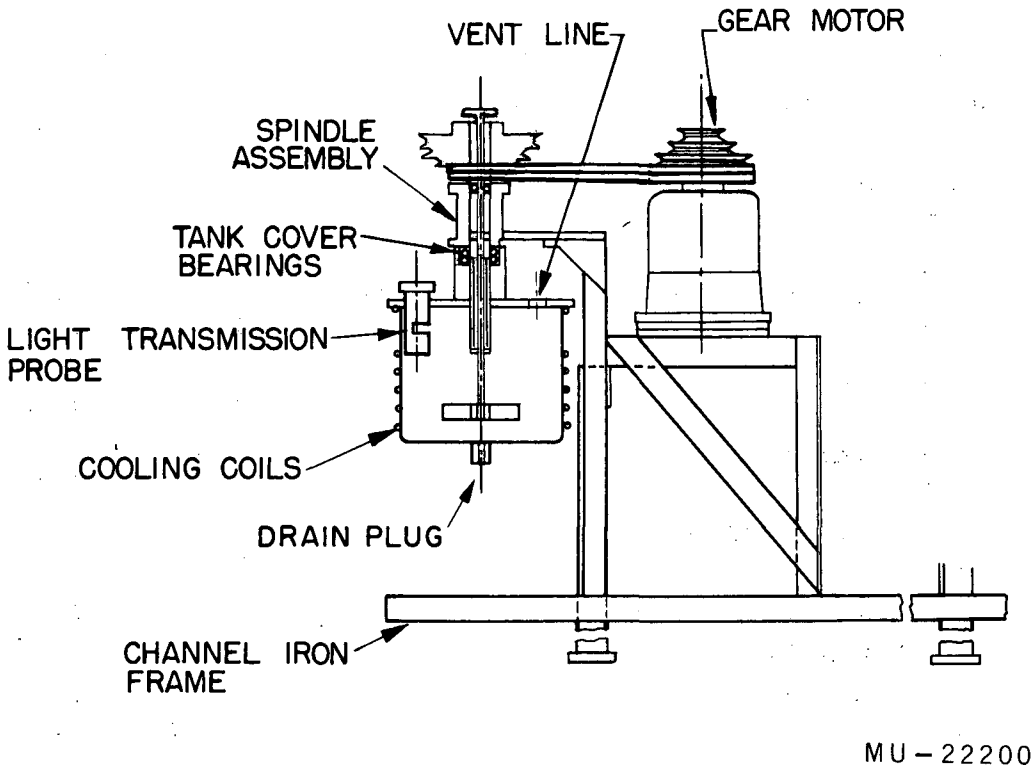

Fig. 2. Stand for mixing tank.

Table I. Physical properties of liquid-liquid systems*

Liquid-liquid System	Refractive Index, n_D^{20}	Density gm/cm^3	Viscosity centipoises	Interfacial Tension (dynes/cm)
Methyl isobutyl ketone (MIBK)	1.3961	0.795	0.59	10.5
Water	1.3347	0.996	1.00	
White oil	1.4779	0.871	184	55.1
Water	1.3330	0.998	1.00	
Isooctane (2, 2, 4-trimethyl pentane)	1.3910	0.693	0.517	46.9
Water	1.3330	0.998	1.00	
n-Butanol	1.3905	0.838	3.30	1.9
Water	1.3408	0.972	1.28	
Cyclohexanone	1.4453	0.941	2.28	3.8
Water	1.3460	0.987	1.03	
Di-isobutyl carbinol	1.4279	0.804	10.03	17.3
Water	1.3330	0.998	1.00	
Methyl isobutyl ketone	1.3985	0.806	0.65	3.0
Ethylene glycol	1.4291	1.064	15.18	
Carbon tetrachloride	1.4601	1.595	0.98	39.9
Water	1.3330	0.998	1.00	
Carbon disulfide	1.6273	1.265	0.378	35.2
Water	1.3330	0.998	1.00	

*All measurements were made at a temperature of 20.0±0.5°C

sets of ball bearings connected to the impeller shaft was contained in a collar welded to the upper side of the frame. This method of assembly allowed the tank cover and impeller shaft to rotate independently of each other, and enabled the power input to be determined by torque measurement on the tank. The tank was fastened to the cover by wing nuts and L-shaped bolts. The vessel was made liquid-and air-tight by a cork gasket around the edge of the cover and a mercury seal on the impeller shaft. Fittings on the tank included an opening in the cover for mounting the light-transmission probe, and several holes tapped for pipe fittings (usually plugged) of which one was used as a thermometer well.

The impeller was driven by a V-belt drive connected to a 3/4-horsepower, 3-phase, 60-cycle, 220 volt, 216-rpm right-angle ring mounted gear motor (supplied by Electra Motors, Inc.). Step-cone pulleys mounted on each of the impeller shafts and on the motor shaft allowed the impellers to rotate at 1.57, 2.57, 3.33, 4.12, 5.00, and 6.45 revolutions per second.

A coil of 1/4-inch o.d. copper tubing was soldered to the outside of the tank to provide temperature control by circulation of cooling water.

Light-Transmission Measurements

Figure 3 shows the probe that was used in this study. The spatial arrangements of the filament lamp and photocell are identical to the probe used by Langlois et al. (8) in the original calibration study, although the external construction is somewhat different. The probe, made of brass, was 8 inches in length and could thus traverse vertically the entire upper half of the mixing tank. By the use of an activator compound (Ebonol-C, manufactured by Ethone, Inc., New Haven, Conn.) it was possible to coat the brass probe in the photocell region with a black copper-oxide coating. This was done to minimize the reflectivity. Shielded cable leads were used for both the filament and the photocell circuits.

The photocell circuit employed (Fig. 4) was essentially the same as described by Vermeulen, Williams, and Langlois (14). However, the galvanometer formerly used as replaced by a continuous recording microammeter (Leeds and Northrup Speedomax, Type G, Model S with amplifier 1010-58-S). This recorder was equipped with both 0.1 and 1.0 microampere ranges. As in the previous study, the current output from the photocell was split by use of two 100,000-ohm decade resistance boxes, one in series and one in parallel with the recorder. The initial I_0 readings (for clear single phases) varied between 0.75 and 1.0 microamperes.

Inherent in photocell readings in an agitated liquid-liquid system is a fluctuation of the I-value reading due to the sensitivity of the recorder to the passage of individual droplets through the probe. This fluctuation varies from system to system, and can make it difficult to measure the most representative value of light transmission. To dampen this fluctuation, a variable capacitance was inserted in the photocell circuit, with a switch to provide settings of 0, 4, 8, and 16 microfarads. The I-value then recorded by the recorder was the mean of the fluctuating values.

The filament circuit providing the light source for the photocell is exactly the same as was used by both Langlois and Fick. The lamp itself was an ordinary penlite lamp rated at 2 volts, and had a built-in lens with which to collimate the light into a parallel beam. However, great care had to be taken to ensure that the lamp-filament and the collimating lens were directly in line, so that a straight parallel beam of light would impinge on the photocell. On the average, one out of thirty lights tested satisfied this requirement.

A gas-filled photocell was used, RCA 1P41, because of its conveniently small size. It was found that, for a constant light source, a certain amount of drift occurred in the photocell current reading, which was characteristic of each individual cell and the level of current drawn. For the photocell used, the drift was usually in the vicinity of 0.0002 microamperes per minute.

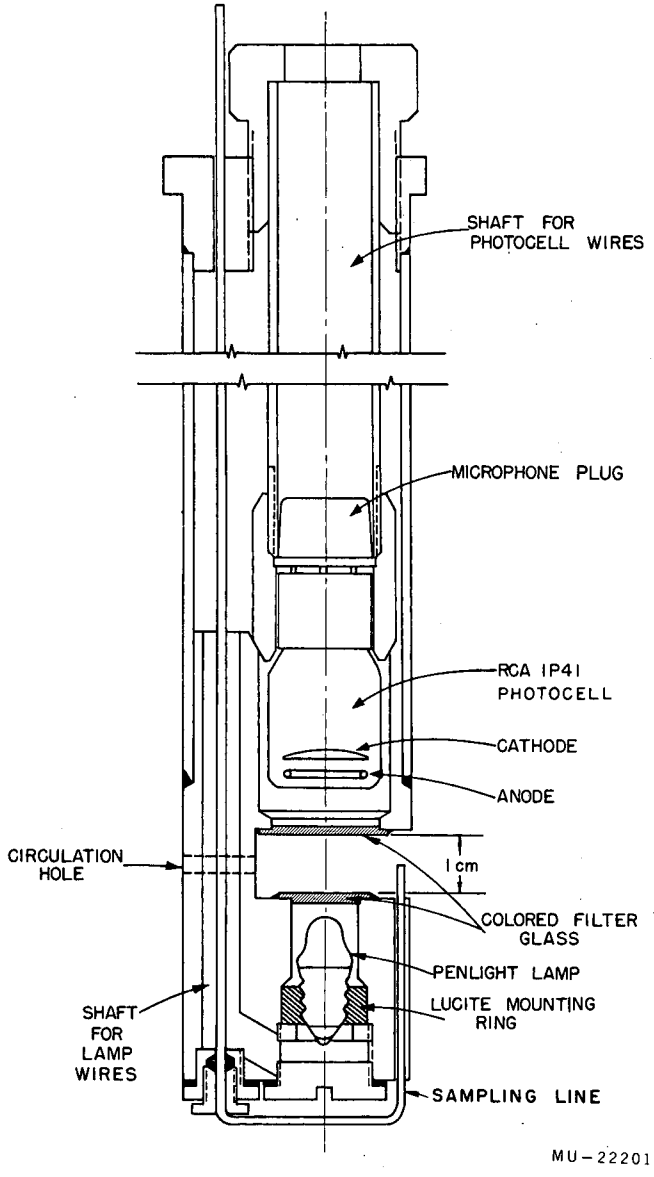

Fig. 3. Photoelectric probe.

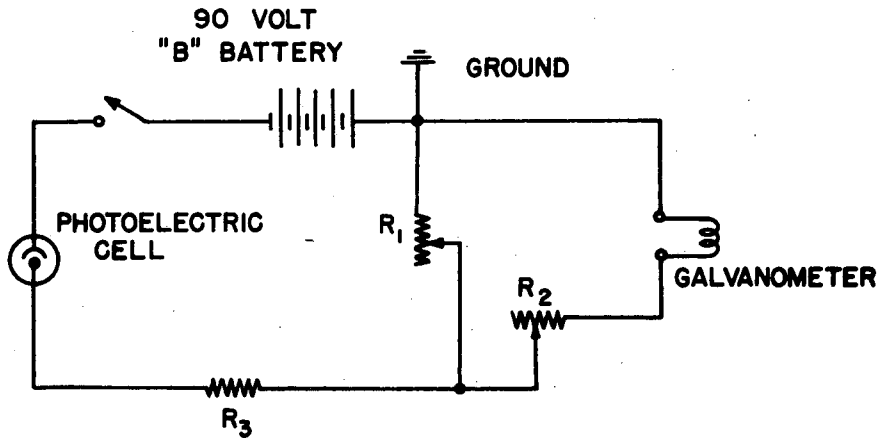

R_1 & R_2 ARE 100,000 OHM DECADE BOXES
R_3 = 200,000 OHM RESISTANCE

MU-5103

Fig. 4. Photocell circuit.

The probe used in the present study was calibrated using the standard mixture compositions for which photographs had been taken by Langlois (2). Since the fixed rotational speeds available in the present equipment were not the same as the speeds used by Langlois, the I_0/I values newly obtained (at the measurable speeds) were cross-plotted, and the extinction ratios at the desired speeds were obtained by interpolation.

These extinction-ratio values were plotted against the specific area values given by Langlois, to determine the slope factor β corresponding to Eq. (1). Four of resulting plots are given as Figures 20-23 in the appendix; the results are summarized in Table II.

In order to plot β, a search was made for a suitable function of m to serve as the independent variable. The ratio $|(m^2-1)/(m^2+2)|$ was suggested by Trice and Rodger, (12), but not supported by any experimental data for $m < 1$; this ratio is significant theoretically for particle diameters smaller than the wavelength of light, but not for those appreciably greater. For large transparent spheres, the scattering distribution depends upon the ratio $|m-1|/(m+1)$, and the angular distribution is independent of which of the phases is continuous, as indicated by van de Hulst, (6). However, some light is totally reflected out of the main beam, with m less than 1. This means that the extinction ratio for systems measured with any given probe tends to be greater when m is less than 1, and will be some function of m (as well as of $|m-1|/(m+1)$. Langlois's data fit the empirical combination $|m-1|/(m+1)|m^{3/2}|$; and the present data are therefore plotted on this basis in Fig. 5. The differences in slope in the higher range may be due to minor differences in probe geometry, between Langlois's unit and the present one.

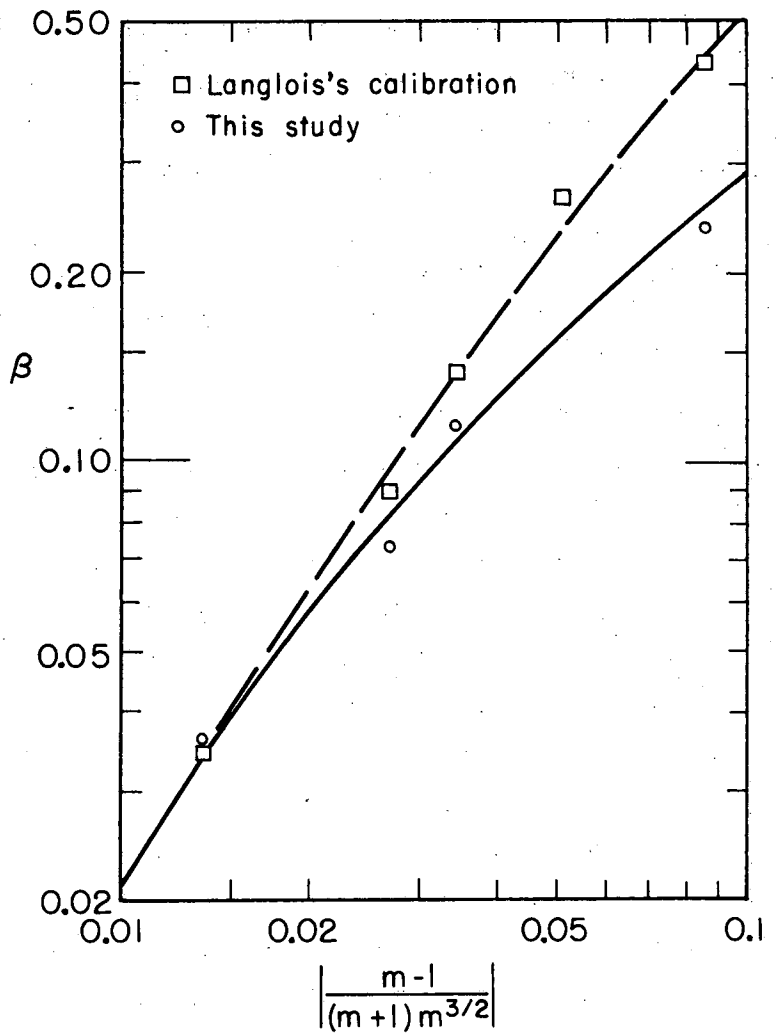

MU-22282

Fig. 5. Calibration curve for specific area measurements.

Table II. Slopes of Extinction Ratio-Specific Area Plots

Dispersed Phase	Continuous Phase	Refractive Index Ratio $m=n_d/n_c$	$\left\lvert \frac{m-1}{(m+1)m^{3/2}} \right\rvert$	Langlois's Slope	Present Slope
Isooctane	Water	1.044	0.0136	0.0346	0.036
Carbon tetrachloride	Water	1.096	0.0270	0.090	0.073
Water	Carbon tetrachloride	0.913	0.0343	0.139	0.114
Carbon disulfide	Water	1.221	0.0509	0.267	—
Water	Carbon disulfide	0.819	0.0866	0.415	0.233
Air	Glycerol	0.685	0.2070	0.913	—

OPERATING PROCEDURE

In preparation for a run, the tank was detached from the steel frame and thoroughly cleaned. After cleaning, the tank was rinsed with one of the liquids to be used; in most cases, distilled water. The tank was then reinstalled on the steel frame and charged with appropriate volumes of the two liquids under investigation. Since many of the liquid pairs used in this study showed some mutual solubility, the liquids were pre-equilibrated before they were charged to the mixing tank.

In each run, it was necessary to ensure that uniform mixing had been achieved. This was done by taking volume-fraction measurements at the bottom, center, and top of the tank. These samples were obtained by drawing out 10 ml of the emulsion through a small stainless steel tube with a syringe. The sample was then centrifuged to separate out the two phases. If all three samples did not agree to within 10%, the run was discontinued. Poor mixing was observed for systems having a relatively large density difference between the two charged liquids, when they were run at low speeds. Also, the combination of low speeds and more highly viscous liquids resulted in poor mixing.

For runs where $\phi = 0.40$, it was necessary to ascertain whether or not the liquid present in the smaller proportion was actually the dispersed phase. This was done by taking conductivity measurements in the following manner. An electrode which was insulated from the tank was inserted into the liquid medium. A potential of 1 to 5 volts was applied between the electrode and the tank. By vertical positioning of the electrode, it was possible to determine the conductivity of the two immiscible liquids on a microammeter. Then, under mixing conditions, the microammeter would indicate directly which phase was continuous. For all the systems studied, the dispersed phase was the liquid charged in the smaller proportions.

Profile measurements were made at five probe locations (designated A, B, C, D, and E) as shown in Figure 1. Because the probe has an appreciable volume, it was necessary to add or withdraw proport-

ionate amounts of the two phases whenever the probe was raised or lowered. The preferred method involved starting with the probe in the uppermost position (E).

After a steady state was reached, and while the mixer was still running, the probe was carefully pushed downward to each subsequent location, thus displacing a volume of emulsified liquid-liquid mixture into an overflow line. In this manner the entire profile was obtained within 15 minutes, without interrupting the agitiation. The speed of operation minimizes the effect of photocell drift. After each run, the input volume fraction was confirmed by emptying the tank and measuring the volume recovered for each phase.

Measurements of the physical properties of the liquid-liquid mixtures were made before and after each run. Interfacial tension was measured by a DuNouy-type interfacial tensiometer, and viscosity measurements were made in an Ostwald viscometer. Refractive index was determined in an Abbé refractometer. Temperature of the agitated liquid-liquid systems was maintained at 20°C by controlled circulation of water through the cooling coil soldered on the outside of the tank.

Sources of Error

Installation of the continuous recorder has improved the sensitivity of photocell readings, so that differences of drop diameters as small as 0.0003 cm. can be identified. The continuous recorder has served to identify certain systems which seemed never to reach a steady state of mixing, but decayed to progressively lower photocell readings in a continuous manner. This behavior was shown by carbon tetrachloride-water and isophorone-water systems. Physical analysis of these systems showed no measurable trend in interfacial tension. It was observed, however, that both these solvents seemed to corrode the stainless steel tank and dissolve the blackening agent of the probe. Consequently data on these systems were not used for the coalescence study. The reproducibility of photocell readings of the other systems was fairly good; Figure 6 includes two duplicate runs on methyl isobutyl ketone in water. The major cause of deviations in reproducibility of runs appears to be the effect of trace impurities.

RESULTS AND DISCUSSION

Variation of Drop Diameter with Probe Position

Clay (3) describes coalescence as resulting from fulfillment of two conditions: (1) that a collision of two droplets occurs; and (2) after once colliding, that they will coalesce. If the geometrical variables are held constant, the collision frequency will be function of the volume fraction of dispersed phase, and both it and the coalescence probability will depend upon the power input, the interfacial tension, and the viscosities. One of the main purposes of this study has been to determine in a quantitative manner the dependence of coalescence on the above-named variables, for a constant agitator geometry.

Table IV lists the drop-size data obtained in the present investigation. Figures 6 through 9 illustrate typical drop-size profiles. The distances represented along the abscissa for probe locations A, B, C, D, and E were obtained by measuring the distance from a point on the tip of the impeller midway between the upper and lower edge to a point on the vertical axis of the light probe centered in the slit opening of the photocell. The intercept on the ordinate axis of the profile curves is taken to be the equilibrium drop size calculated from a modified correlation of Langlois's work;

$$d_0/L = 0.055 f'_\phi \; N_{We}^{-0.60} = 0.055 f'_\phi \left(\frac{N^2 L^3 \bar{\rho}}{\sigma} \right)^{-0.60} . \qquad (9)$$

Here f'_ϕ is slightly different from the factor f_ϕ in Eq. (2a), in regard to the reference diameter (now at zero volume fraction) and to relative slope:

$$f'_\phi = 1.00 + 2.5\phi_d \qquad (10)$$

Several interesting qualitative conclusions can be deduced from the plotted profile curves. First, there is no simple functional dependence, on volume fraction, of the amount of coalescence occurring be-

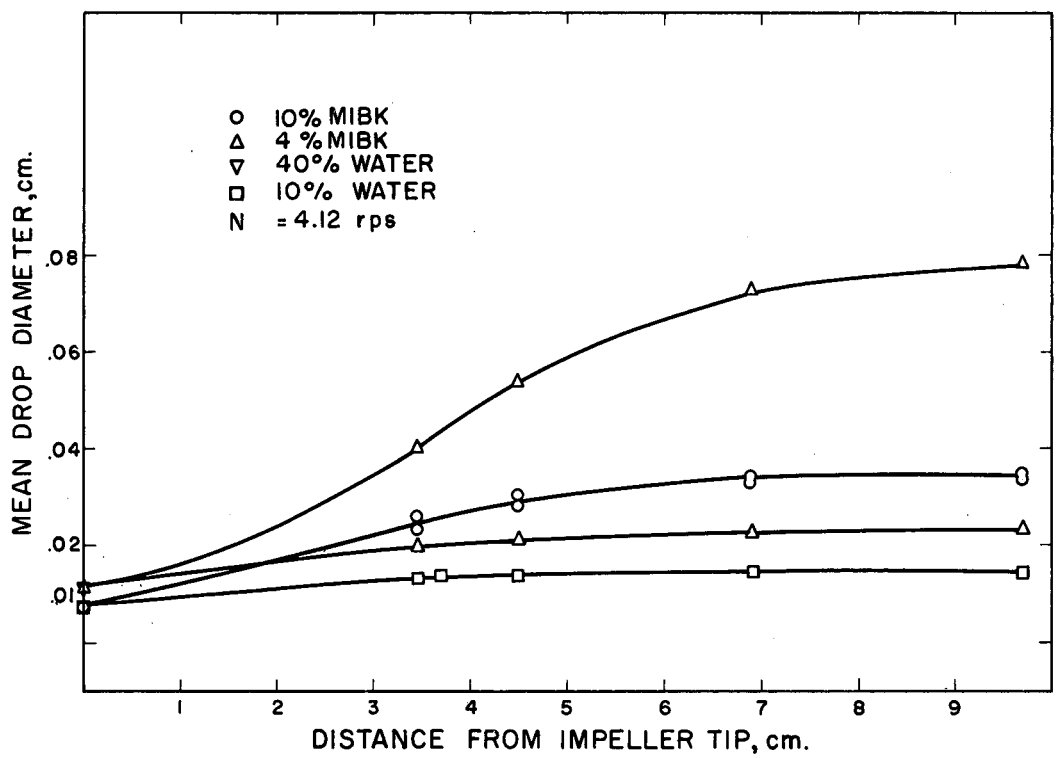

MU-16059

Fig. 6. Drop-diameter profile for methyl isobutyl ketone water mixtures.

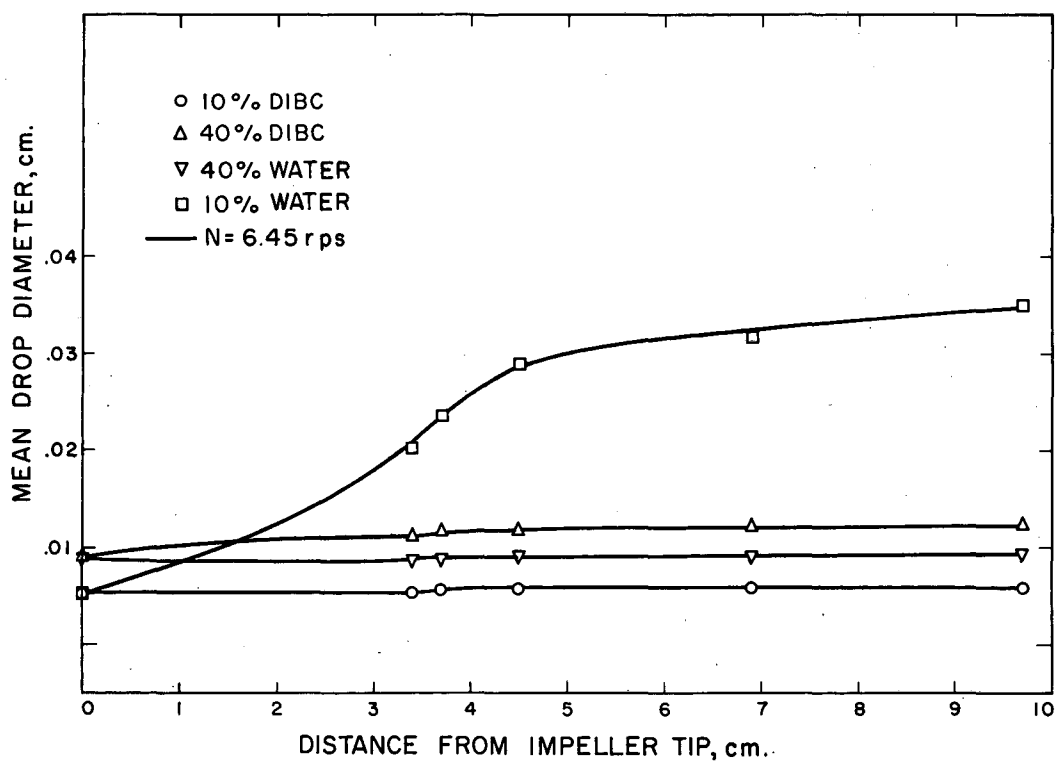

MU-16060

Fig. 7. Drop-diameter profile for di-isobutyl carbinol-water mixtures.

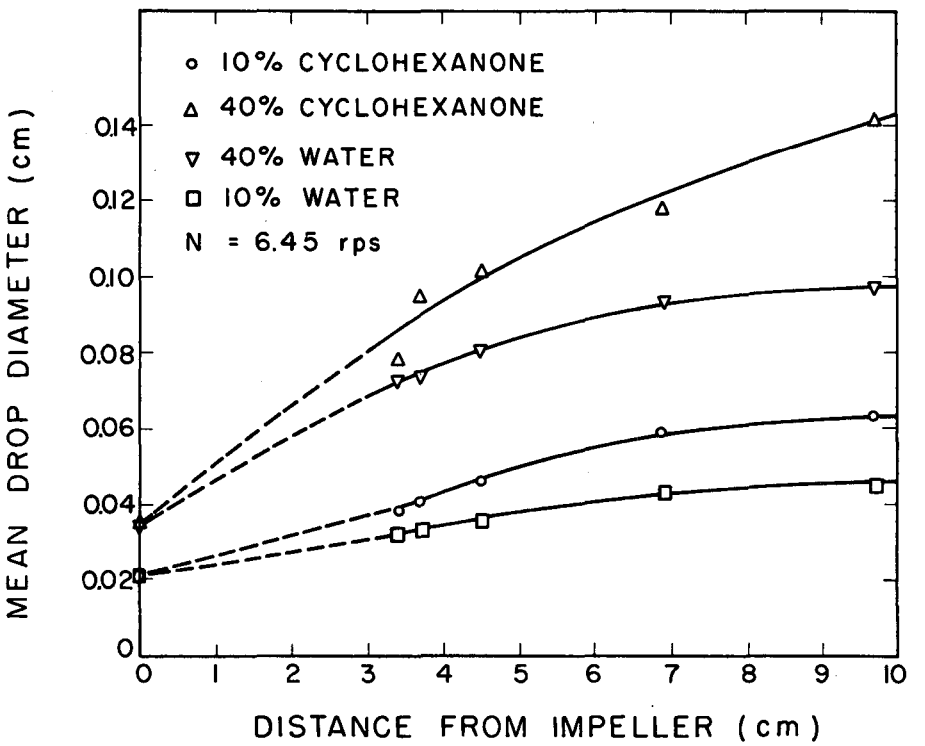

MU-22192

Fig. 8. Drop-diameter profile for cyclohexanone-water mixtures.

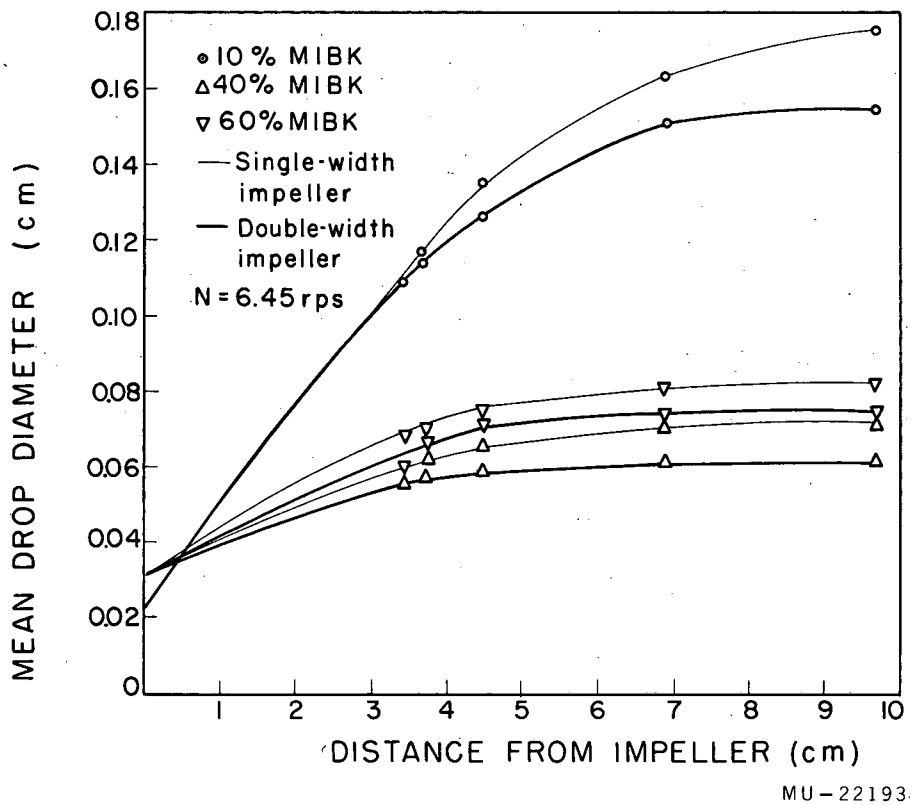

Fig. 9. Drop-diameter profile for methyl isobutyl ketone–glycol mixtures.

tween the impeller tip and the uppermost probe position E. The cyclohexanone-water systems (Fig. 8) show a straightforward relationship; here the amount of coalescence is directly proportional to the volume fraction. On the other hand, curves for the MIBK/water and MIBK/glycol systems (Figs. 6 and 9), exhibit coalescence behavior entirely different from this. MIBK-in-water (10% and 40% MIBK) shows more coalescence than water-in-MIBK; the system having 40% MIBK dispersed shows the greatest diameter increase. The MIBK-in-glycol system also shows more coalescence than glycol-in-MIBK.

The comparison of the coalescence curves for 10% and 40% MIBK dispersed is in itself very interesting. The degree of coalescence in the 10% MIBK system yields a mean drop diameter at point E which is greater than that observed for the 40% MIBK system at the same point. This is in direct opposition to what would be predicted from consideration of an equilibrium relation alone, such as Eq. (9).

There is one marked consistency in the behavior of these systems: when the ratio of continuous-phase viscosity to dispersed-phase viscosity is much greater than one, more coalescence occurs. This effect is still more pronounced for 10% dispersed than for 40% dispersed. Also, for systems where μ_c/μ_d is close to unity and the interfacial tension relatively high (35-50 dynes/cm), no appreciable drop-size variation is observed. The isooctane/water and carbon tetrachloride/water systems exemplify this behavior.

Correlation

Because of physical limitations it has not been possible to obtain data on drop size between point A in the tank and the impeller tip. Since this interval is appreciable when compared to the total distance spanned, it seems quite reasonable that a significant degree of coalescence occurs in this interval. It is therefore proposed to correlate the observed coalescence as a function of its inherent independent variables, and then to use this relation as a means for predicting drop sizes from the impeller tip to any point in the tank.

Because of the varied coalescence behavior of the different systems in the interval A to D, it was decided to attack the problem by means of a linear regression analysis. The variables that were considered important are:

1. Weber number, $N_{We} = N^2 L^3 \rho_c / \sigma$
2. Reynolds number, $N_{Re} = N L^2 \rho_c / \mu_c$
3. Density-difference ratio, $\Delta\rho / \rho_c$
4. Viscosity ratio, μ_c / μ_d
5. Viscosity--volume-fraction function,

$$\psi = \left(\frac{\mu_c}{\mu_d} \phi_d^x + \frac{\mu_d}{\mu_c} \phi_c^x \right).$$

The function ψ (psi) was used in an attempt to explain the viscosity and volume-fraction effects on the coalescence found in the MIBK/glycol and butanol/water systems. The exponent x was varied from 0 through 3.0.

First Correlation.

With the use of an IBM-650 computer, many regression runs were made on the data, changing the different variables and the exponent value. The different runs consistently showed a negligible contribution from variables (3) and (4) above. The optimum function, with a correlation coefficient of 0.72, is as follows for Δ_{A-D}, the coalescence measured between points A and D:

$$b_{A-D}\Delta/L = 1.30\times10^{-4}\, N_{We}^{-0.45}\, N_{Re}^{0.50}\left(\frac{\mu_c}{\mu_d}\,\phi_d^{2.5} + \frac{\mu_d}{\mu_c}\,\phi_c^{2.5}\right)^{-0.70}\phi_d^{0.30} \tag{11}$$

This relation is shown in Fig. 10.

By using a combination of a coalescence function and an equilibrium-drop-size function, a relation can be found which would predict a mean drop diameter at any point in the tank. A general form of this relation is;

$$d_i = d_0 + b_{0-i}\Delta \tag{12}$$

where d_i is the drop diameter at point i (e. g., points A and D in the present study); d_0 is the drop size at the impeller tip, termed the equilibrium drop size; Δ is a function of the same form as Eq. (11); and b_{0-i} is a numerical coefficient which is a function of direction and distance from the impeller tip to the point in question (b_{0-A} or b_{0-D}, in the present study).

Two main assumptions are involved in this model. They are:

1. The equilibrium drop size (d_0) is a function of $(N_{We})^{-0.6}$, as theoretically predicted by Hinze (6) and experimentally determined by Langlois. The function is expressed:

$$d_0 = a_0 f'_\phi\,(N_{We})^{-0.6} \tag{13}$$

where a_0 is the equilibrium-drop-size constant, assumed the same for both Langlois's and the present data; and the volume-fraction function is expressed as $f'_\phi = 1 + c\phi$ where c is a constant to be determined.

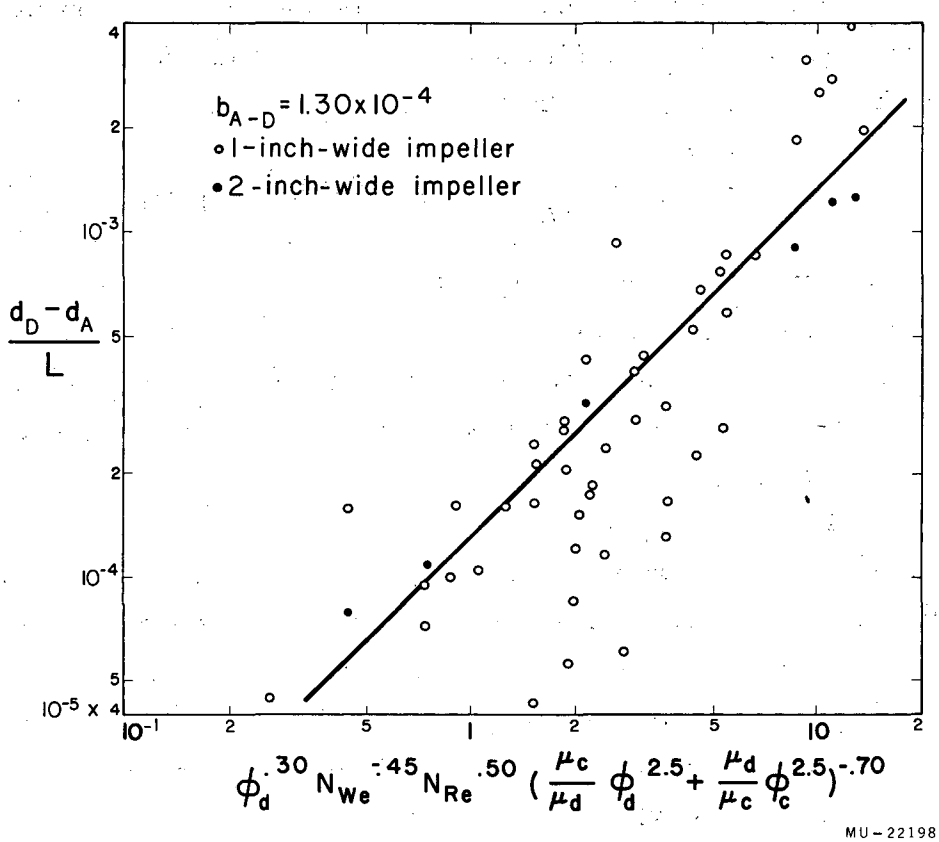

Fig. 10. Correlation for coalescence between locations A and D.

2. The nature of the coalescence function does not change from one point to another.

The determination of the optimum c, b_{0-A} and b_{0-D} was done by a trial-and-error calculation. The two equations used are

$$d_A/L = a_0(1 + c\phi)N_{We}^{-0.6} + b_{0-A}\Delta \tag{14}$$

and

$$d_D/L = a_0(1 + c\phi)N_{We}^{-0.6} + b_{0-D}\Delta \tag{15}$$

Calculations were performed first for the data at the D position. Values for c and a_0 were assumed and a set of b_{0-D} values were calculated for each measurement. The average b_{0-D} was then used to calculate predicted d_D's for all the data. The sum of the square of differences between the actual and predicted drop size was determined. By minimizing this sum as a function of different assumed c's and a_0's, an optimum function could be found for describing the experimental data. This function turned out as follows:

$$d_D/L = 0.055(1 + 2.5\phi)N_{We}^{-0.6} + 3.80\times10^{-4}\Delta \tag{16}$$

Using these newly determined equilibrium constants for c and a_0 (2.5 and 0.055 respectively), b_{0-A} can quickly be found for the data obtained at position A. The optimum b_{0-A} is 2.4×10^{-4}. Figures 11 and 12 show the fit to Eq. (15) or (16); and Figs. 13 and 14 the fit to Eq. (14). Since the coalescence function Δ is assumed to be independent of the distance from the impeller tip, the difference of b_{0-D} and b_{0-A} is equal to b_{A-D}. This difference is 1.4×10^{-4} and compares reasonably well with the value obtained from the original regression analysis, 1.30×10^{-4}.

Extension to Earlier Studies.

Even though impeller drop sizes were measured closer to the impeller tip in Langlois's work than in the present study, it is believed that some coalescence occurred in the interval. Accordingly, the same drop-size model (Eq. 12) was assumed for his data, to see if the proposed coalescence model is again applicable. The same type of trial-and-error solution was used, except that $c = 2.5$ was fixed and only a_0 and b_{0-L} were determined. The result for a_0 was similar to that found for the coalescence data (as expected, since the same size of tank and the same impeller type were used in both studies). The resulting modified b_{0-A} and b_{0-D} were calculated. (The value reported above for a_0 is the result of this adjustment.) The final relation describing Langlois's points is as follows:

$$d_L/L = 0.055 \; f_\phi \; N_{We}^{-0.6} + 0.71\times10^{-4} \; \Delta . \tag{17}$$

The results of Eq. (17) are plotted in Fig. 15.

Langlois's original correlation (8) had a value for $a_0 = 0.083$, with $f_\phi = 0.75 + 2.5\phi$ constituting a larger relative ϕ effect. The scaledown of d_0 in the present study due both to c and to coalescence is, on the average, 0.83 of the d_0 used by Langlois. A readjusted a_0, for purposes of comparison with the present study, is thus 0.083 (0.83) = 0.069. The difference between 0.055 and 0.069 represents the volume-fraction effect between $\phi = 0.1$ and $\phi = 0$. This amount of coalescence is not enough to invalidate the -0.6 exponent on the Weber number. The effect of this scaledown on the original correlation, for d at $\phi = 0.1$, is shown in Fig. 16.

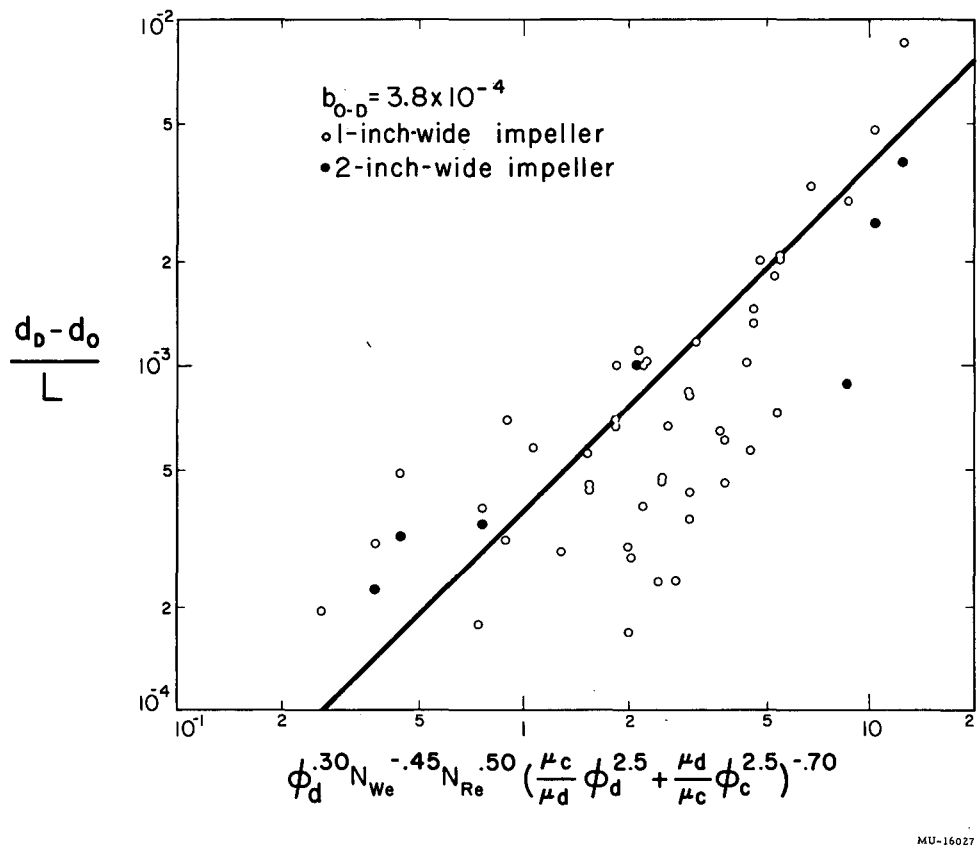

Fig. 11. Correlation for coalescence between impeller tip and location D.

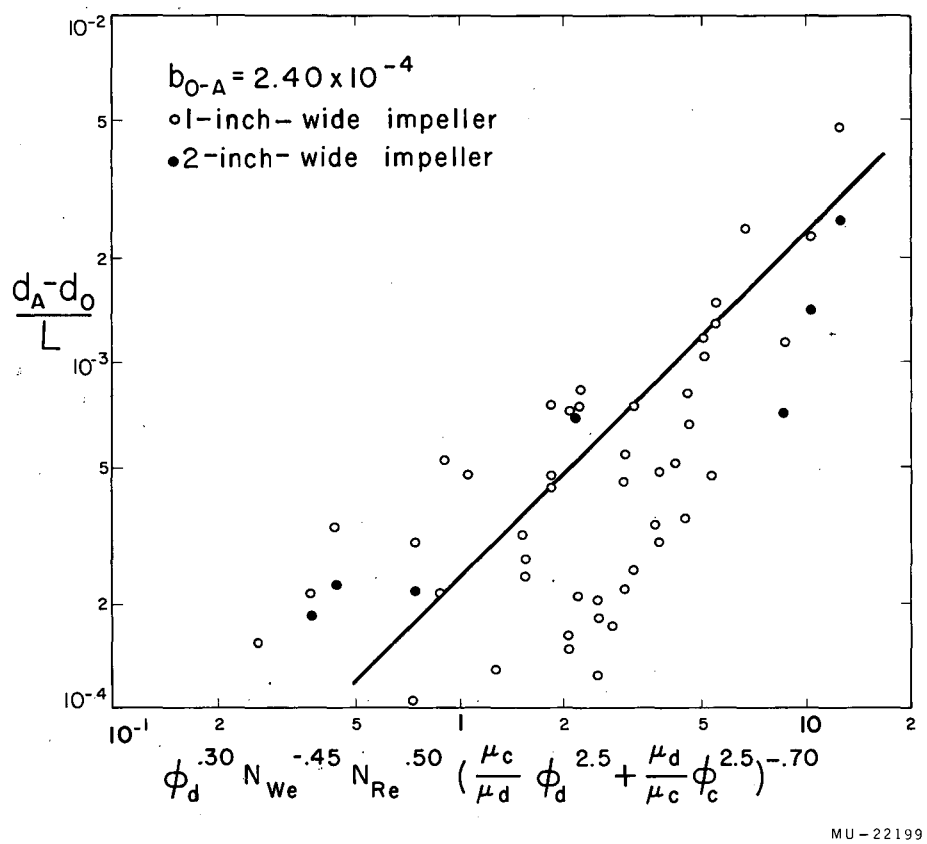

Fig. 12. Comparison of calculated and measured drop diameters at point D.

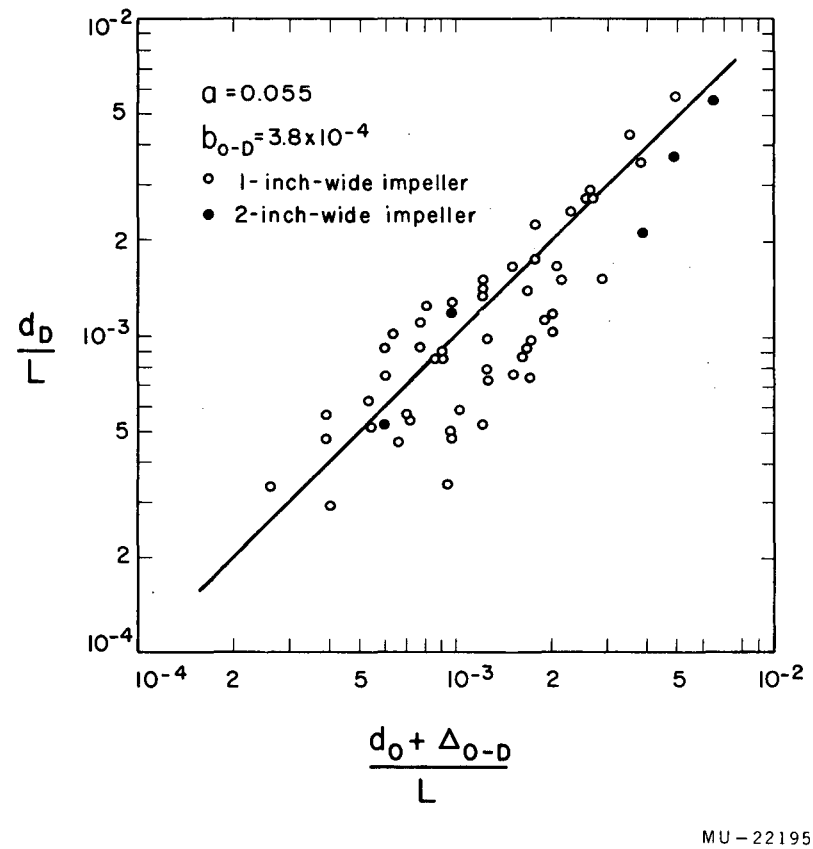

Fig. 13. Correlation for coalescence between impeller tip and location A.

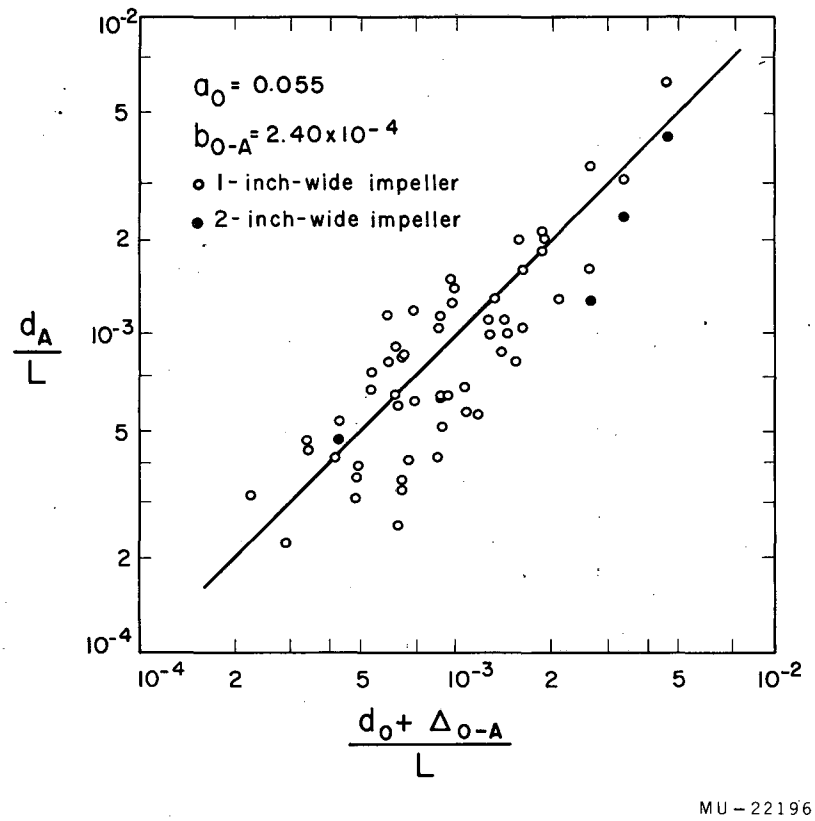

Fig. 14. Comparison of calculated and measured drop diameters at point A.

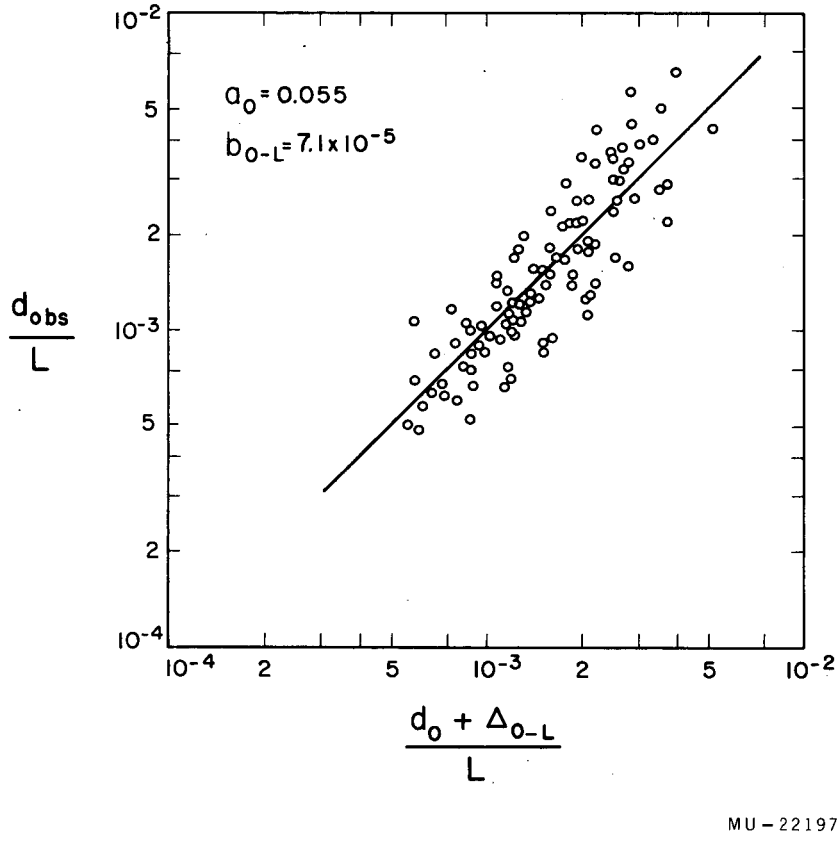

Fig. 15. Comparison of calculated and measured drop diameters for Langlois's data.

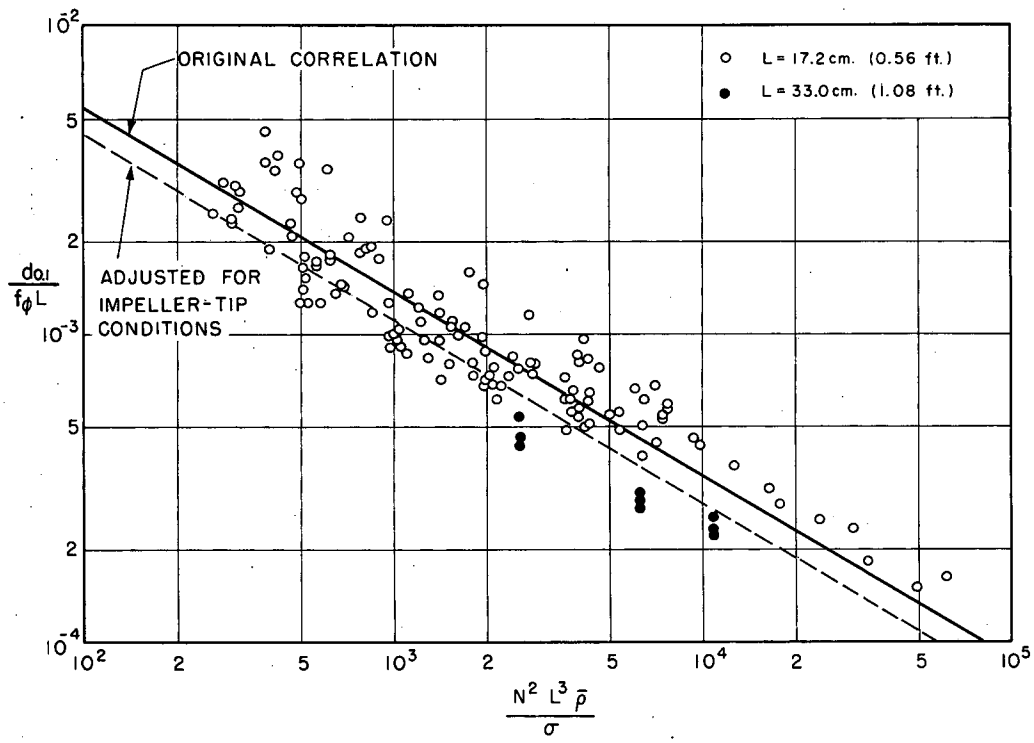

Fig. 16. Weber-number dependence of mean drop diameter, at $\phi = 0.1$, adjusted to impeller tip.

Runs with Double-Width Impeller.

Some coalescence runs were made with an impeller having a blade width (W) of 2.0 inches. As can be seen in Fig. 9 for the MIBK/glycol system, the coalescence is less for this impeller than it is for W = 1.0 inch. However, the precision of the present coalescence relation is not great enough to correlate this difference, and these points can be plotted on the same curve (Fig. 10).

Mixture-Viscosity Correction.

Shinnar and Church, in a theoretical study of droplet breakup under different limiting conditions (11), find that coalescence probably involves an "adhesive energy" rather than a true interfacial tension. It seems likely that the empirical viscosity--volume-fraction function, ψ, which has proved particularly necessary to account for the experimental behavior of the MIBK systems, contributes (along with σ) to the effective adhesive energy.

We have investigated the possibility that an already-known function of viscosities, such as the effective viscosity of the mixture, could be used to replace ψ. The mixture viscosity has been given by Vermeulen, Williams, and Langlois (14) as

$$\mu_m = \frac{\mu_c}{1-\phi_d}\left[1 + \frac{1.5\,\phi_d\mu_d}{\mu_c + \mu_d}\right] . \tag{18}$$

Reference to work of Vand (13) on dispersions of solid spheres, for which μ_d is infinite, shows that this equation gives insufficient correction. We have therefore altered the form of the relation, to yield:

$$\mu_m = \frac{\mu_c}{(1-\phi_d)^{3/2}}\left[1 + \frac{\phi_d\,\mu_d}{\mu_c + \mu_d}\right]^{3/2} . \tag{19}$$

Unbaffled tank studies by Laity and Treybal (7) confirm the use of this general type of expression, but only in certain cases. For other cases, possibly involving internal circulation of droplets, the effective mixture viscosity is less than the value for the continuous phase alone. In any event, the result of this study was that use of μ_m/μ_c from this relation, as a multiplier for separate viscosity-ratio and volume-fraction terms, proves not to have the same correlating effect as the ψ term. It appears that any real improvement over the ψ treatment will have to await more precise experiments, or a more complete theoretical definition of the adhesive energy.

Second Correlation. The coalescence relations given in Eqs. (11) - (17) involve a -0.40 exponent on impeller speed, contributed to from a -0.45 exponent on Weber number and a +0.40 exponent on Reynolds number. Although the -0.40 power is marginally better than higher values on the basis of linear-regression analysis, individual runs appear to show a somewhat higher dependence on speed (as does the work of other investigators, reported in the next section).

When the speed dependence is altered to a -0.65 power, substantially the same correlation coefficient (0.69) is obtained. The results of this treatment, plotted in Figure 17, correspond to the following relation:

$$\frac{d_D - d_A}{L} = \frac{b'_{A-D}\,\Delta'}{L} = 1.60\times10^{-3}\, N_{We}^{-0.45}\, N_{Re}^{0.25}\, \psi^{-0.70}\, \phi^{0.30} \,. \tag{20}$$

It follows that Eq. (12) can be applied in the revised form:

$$d_i = d_0 + b'_{0-i}\,\Delta'_i \tag{21}$$

with values of $b'_{0-A} = 3.0\times10^{-3}$, $b'_{0-D} = 4.6\times10^{-3}$, and (for Langlois's data) $b'_{0-L} = 0.88\times10^{-3}$. This treatment is belived to be more suitable than the first correlation, for extrapolation purposes.

Comparison with Rodger's Results

The present and previous studies in this Laboratory show the equilibrium drop size d_0 to be a function of the Weber number of the -0.6 power; this is in agreement with Hinze's analysis of Clay's data (3, 5). However, Rodger, Trice, and Rushton (9) reported a -0.36 exponential dependence on Weber number, or a -0.72 dependence on agitator speed; and Shinnar and Church (11) have predicted a -0.75 speed dependence for coalescence.

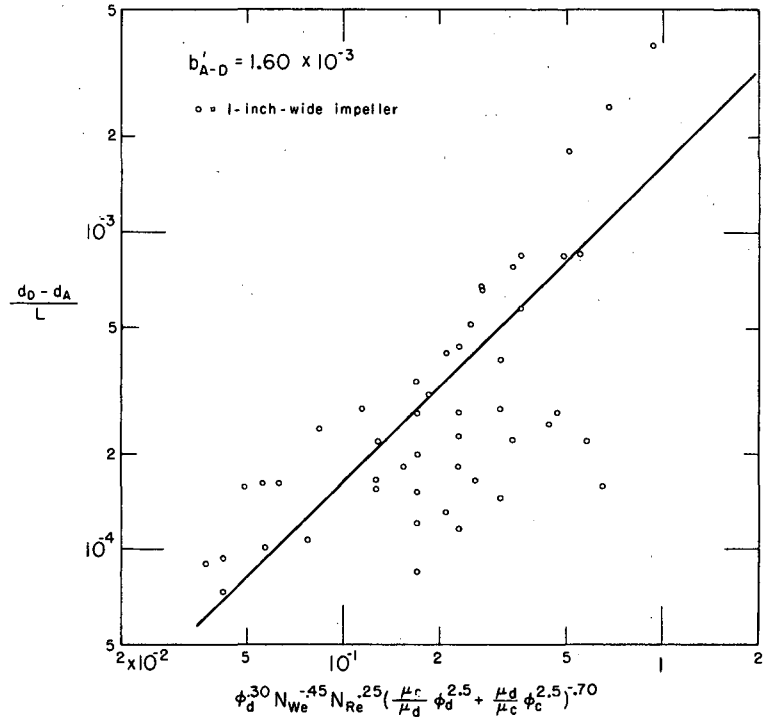

Fig. 17. Second correlation for coalescence, between impeller tip and location D.

The drop-size measurements of Rodger et al. were obtained at the bottom of the mixing tank, with a sizeable gap between the impeller tip and the point of measurement. Two other main differences in equipment were as follows: The present probe is of a different design and much larger, and a 4-blade paddle was used rather than a 6-blade disk-type turbine. However, the power requirement for paddles and for turbines appears to be essentially the same for a given blade-tip geometry (overall diameter, and blade width); hence, a correction needs only to be made for the number of blades. All of Rodger's data were obtained at $\phi = 0.50$, using only water as the continuous phase.

It appears that the difference in the Weber-number exponents can be explained by Rodger's having measured drops that had undergone considerable coalescence. Rodger's correlation can be put in the form:

$$d_R/L = K\, N_{We}^{-0.36} (\mu_c/\mu_d)^{0.2}\, f(\phi, t, \Delta\rho/\rho_c) \tag{22}$$

where t is an experimental settling-time ratio (relative to unit time).

The increase in power has been observed to be slightly less than proportional to the increased number of blades (10). Thus a 6-blade turbine in a buffled tank consumes around 1.36 as much power as a 4-blade impeller of the same blade-tip geometry. Also, from Eqs. (3) and (5), we find that d_0 is proportional to $(P)^{-0.4}$. Hence, for Rodger's experimental conditions, we estimate that

$$d_0/L = 0.0485\, f'_\phi\, N_{We}^{-0.60} \tag{23}$$

In most of the cases they studied, the difference $d-d_0$ is substantially larger than d_0.

In the work of Rodger, Trice, and Rushton, measurements were made of several impellers in each mixing vessel, with each being run at several speeds. These data are thus quite sensitive to the variation in speed. When an impeller-tip diameter (dependent on the -1.2 power of speed) is subtracted from the total, the remainder is found (quite reasonably) to have a smaller dependence than the -0.72 power observed

for the total. The dependence of the increment is, in fact, the -0.65 power, to within about ± 0.025 on the exponent.

In the same way that ψ was introduced to correct for the difference between adhesive energy and interfacial tension in the preceding treatment, Rodger and coworkers have found it desirable to use the viscosity ratio and the settling-time ratio which appear in Eq. (22). In adapting our correlation to their results, we have retained the ψ group, rather than their viscosity ratio. Also, we have believed it desirable to convert their "relative settling time" into a truly dimensionless group, $(t\sigma/\ell\,\mu_c)$, where ℓ is the settling distance corresponding to the measured time. The resulting correlation has the form

$$\frac{d_R - d_0}{L} = b''_{0-R}\ \Delta'' \tag{24}$$

with $b''_{0-R} = 1.26$, and

$$\Delta'' = N_{We}^{-0.45}\ N_{Re}^{0.25}(\psi')^{-0.70}\ (T/L)^{1.20}(t\sigma/\ell\mu_c)^{-0.40} \tag{25}$$

where $\psi' = (\mu_0/\mu_d) + (\mu_d/\mu_c)$; and T is the tank diameter, for geometrically similar vessels. A plot of this correlation is shown in Fig. 18. The volume-fraction is omitted here because it is always 0.50.

From these results, we conclude that a settling-time measurement may be a necessary step in characterizing the coalescence properties of a system. If so, the relative success of a correlation that does not include it would be explained by the fact that the different systems studied in our investigation all may have had a relatively similar settling-time behavior. The work described in the next section offers a possible alternative for obtaining a time measurement that could be used in describing coalescence behavior.

A complete correlation for the incremental mean drop diameter might therefore depend on the following product of dimensionless groups:

$$N_{We}^{-0.45}\ N_{Re}^{0.25}\psi^{-0.70}\phi_d^{0.30}\ (T/L)^{1.20}(t\sigma/\ell\mu_0)^{-0.40}\ .$$

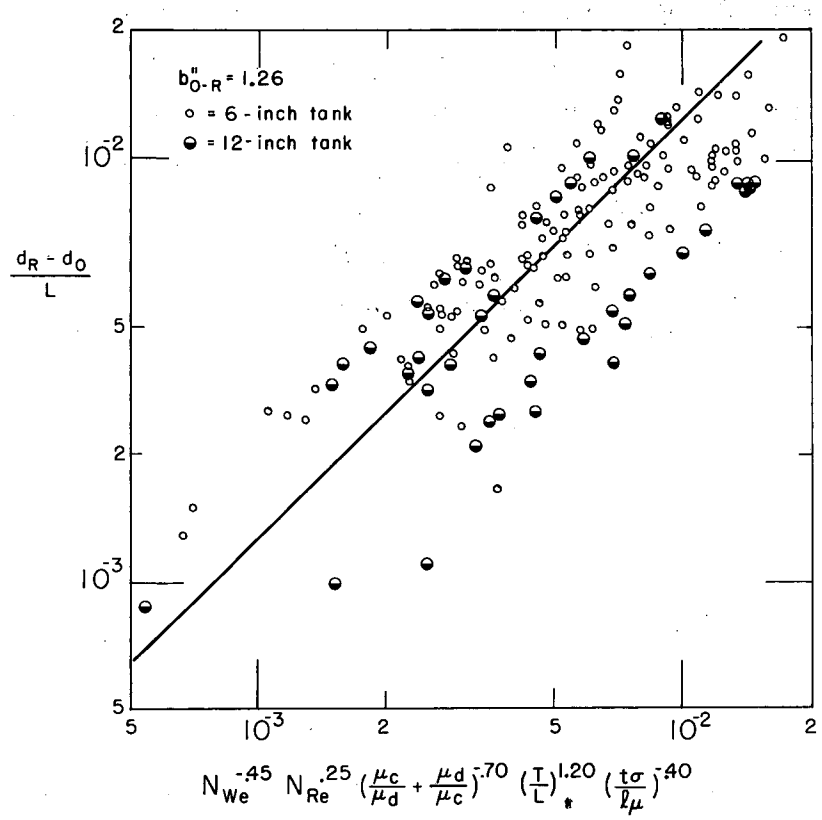

MU-22283

Fig. 18. Correlation of coalescence part of Rodger-Trice-Rushton measurements.

DISPERSION STUDIES

Measurements

The rate of dispersion of an agitated liquid-liquid system was studied by means of injecting into the mixing tank a blue dye, soluble only in the dispersed phase, and then noting the length of time for the dye to disperse uniformly. Variables involved are impeller speed (N), volume fraction (ϕ), and the physical properties of the immiscible liquids. The probe was positioned opposite the impeller tip.

Preparation for a run was done in the manner that has been described for the drop-profile studies. The fastest chart speed (1.0 inch/min.) was set on the recorder. The variable-capacitance switch was turned to zero, to minimize the time constant of the circuit. When the agitated emulsion had reached equilibrium for any given speed, 20 ml of blue dye was injected into the tank downstream from the probe by means of an hypodermic syringe. Immediately the current output of the photocell drifted downward to a new steady-state value, the drift being due to light absorption by the blue dye.

Results

Since the decay curves approximated a first-order behavior, their half-life τ was recorded; Table III gives the results. After each run, a check on the interfacial tension of the two liquids did not reveal any more than 1 to 2% change from the value observed before the run was made. The dyes used were: (1) soluble in organic phase: Sudan Blue and Victoria Blue, obtained from General Dyestuff Co.; and Du-Pont Oil Blue A; (2) soluble in water phase: Patent Blue AF, obtained from General Dyestuff Co.

The best dimensionless fit of the data was obtained when $N\tau$ was plotted against $N_{We}^{-0.6} N_{Re}^{0.2}$, (as shown in Figure 19); with $N_{We} = N^2L^3 \bar{\rho}/\sigma$ and $N_{Re} = NL^2 \bar{\rho}/\mu_m$. Here, μ_m is the viscosity of the emulsion as given by Eq. (10).

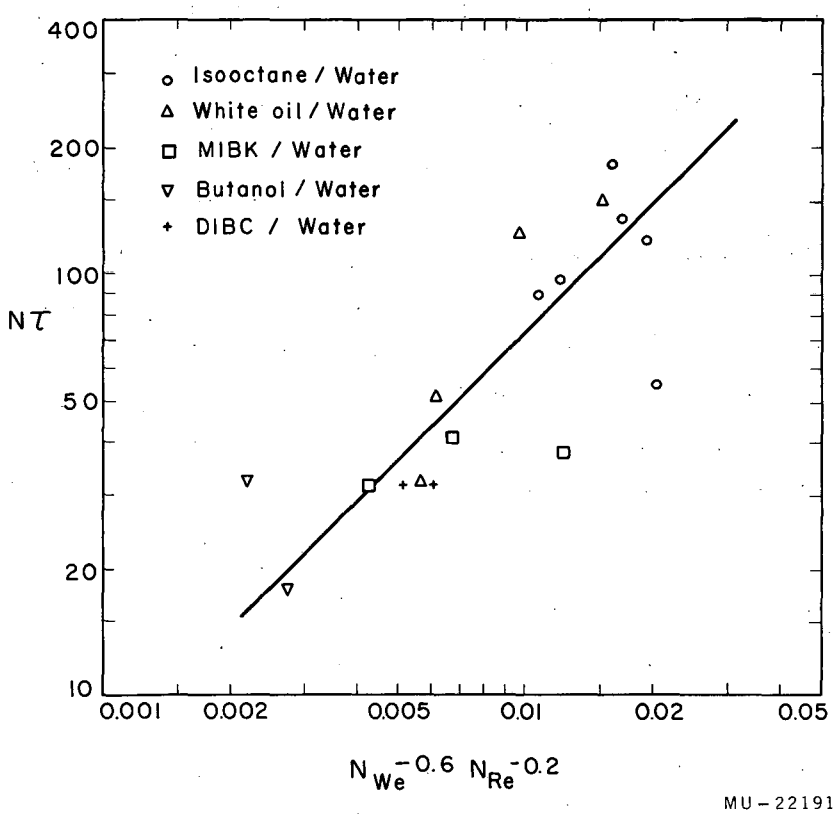

Fig. 19. Dimensionless relation for rate of dispersion.

Table III. Half-life times for mixing of dye tracer soluble only in dispersed phase

System	ϕ	N (rev/sec)	τ (sec)	N_{We}	N_{Re}
Isooctane in water	0.10	3.33	16	412	43,900
	0.20	4.12	45	631	43,800
Water in isooctane	0.10	4.12	30	631	71,900
	0.10	6.45	15	1545	111,250
	0.40	4.12	33	631	38,300
	0.40	6.45	14	1545	60,000
White oil in water	0.10	5.00	30	862	62,800
Water in white oil	0.10	6.45	5	1435	[illegible]443
	0.40	4.12	31	586	[illegible]189
	0.40	6.45	8	1435	[illegible]295
MIBK in water	0.10	2.57	3	1155	33,300
Water in MIBK	0.10	2.57	15	1155	46,500
	0.40	4.12	10	2970	38,400
	0.40	6.45	5	7290	60,200
Butanol in water	0.20	4.12	8	16400	32,500
Water in butanol	0.40	2.57	7	6380	5,420
DIBC in water	0.10	6.45	5	4420	84,200
	0.40	6.45	5	4420	43,500

Although these results are preliminary, certain trends can be observed. A fractional rate of dispersion, k, may be defined as $k = 0.693/\tau$. Since

$$N\tau = 750 \cdot N_{We}^{-0.6} N_{Re}^{0.2} \tag{26}$$

it follows that

$$k = 0.92 \cdot 10^{-3} N (N_{We})^{0.6} (N_{Re})^{-0.2} \tag{27}$$

From Eq. (2), the interfacial area per unit volume of dispersed phase (A/ϕ) is proportional to $N_{We}^{0.6}$, and hence

$$k = 1.28 \times 10^{-5} N (A/\phi) f_{\phi} L (N_{Re})^{-0.2} . \tag{28}$$

Thus k is proportional to (A/ϕ) and, further, to the 0.8 power of N and L.

Up to the present, no direct relation has been established between this mixing phenomenon and the changes of drop diameter just reported.

CONCLUSIONS

a. Many two-phase liquid systems undergoing agitation show a substantial increase in the average droplet size, as the distance from the impeller tip increases. Such systems are often characterized by a high ratio of viscosities of the two phases, and by a relatively low interfacial tension (below 20 dynes/cm).

b. The observed coalescence behavior can be correlated as a function of Weber and Reynolds numbers, dispersed-phase volume fraction, viscosity ratio, tank-diameter/impeller-diameter ratio, and possibly a settling-time group. This treatment also resolves the conflict between the results of Rodger, Trice, and Rushton (5), and studies in this Laboratory.

A = specific area, or total interfacial area per unit volume, cm^2/cm^3.

a_0 = equilibrium drop-size constant.

b_{i-j} = coalescence parameter used to describe coalescence occurring between points i and j.

c = coefficient in f_ϕ' relation, Eqs. (14)-(15).

d_0 = equilibrium drop diameter, cm.

d_A, d_B, d_C, d_D, d_E = drop diameter at locations A, B, C, D, and E respectively, cm.

d_L = Langlois's drop diameter, cm.

$d_i = d_0 + b_{0-i} \Delta \cdot L$ or $d_i = d_0 + b'_{0-i} \Delta' \cdot L$.

d_R = Rodger's drop diameter, cm.

E = power input per unit mass.

f_ϕ = ratio of actual mean drop diameter to diameter at $\phi = 0.10$. (Used in Langlois's study).

f_ϕ' = ratio of actual mean drop diameter to diameter at $\phi \longrightarrow 0$. (Used in present study).

I = light transmission through emulsion, measured as photocell output, microamperes.

I_0 = light transmission through the continuous phase alone, measured as photocell output, microamperes.

I/I_0 = extinction ratio.

k = rate coefficient in dispersion runs.

L = paddle diameter, cm; 12.7 cm in present study; 17.2 cm in Langlois's study.

ℓ = initial emulsion height, in Rodger's settling tests.

m = refractive index ratio, n_d/n_c.

n_c = refractive index (n_D^{20}) of continuous phase.

n_d = refractive index of dispersed phase

N = stirring speed, rev/sec

N_{Re} = Reynolds number for a stirred tank, $NL^2 \rho_c/\mu_c$

N_{We} = Weber group, $N^2L^3\rho_c/\sigma$.

P = power, gm cm^2/sec^3.

T = tank diameter, cm.

t = time to complete coalescence in Rodger's settling tests.

V = volume of flow field, cm^3.

v = velocityfluctuation, cm/sec.

W = width (height) of agitator impeller, cm.

x = exponent.

β = slope of curves of extinction ratio (I/I_0) versus specific area A.

$\Delta = N_{We}^{-0.45} N_{Re}^{u} \psi \phi^{0.30}$, general form of coalescence function, giving amount of coalescence occurring between points i and j. For Δ, exponent $u = 0.50$; for Δ', $u = 0.25$.

μ_c = viscosity of continuous phase, g/(sec) (cm).

μ_d = viscosity of dispersed phase, g/(sec) (cm).

μ_m = viscosity of emulsified mixture(Eqs. 18 and 19).

ρ' = volumetric mean density, g/cm^3.

ρ_c = density of discontinuous phase, g/cm^3.

$\bar{\rho}' = 0.6\ \rho_d + 0.4\ \rho_c$, effective mean density, g/cm^3.

σ = interfacial tension, dynes/cm.

τ = half-life of dispersion process, sec.

ϕ_d = volume-fraction of dispersed phase (or ϕ).

ϕ_c = volume-fraction of continuous phase; $\phi_c = 1 - \phi_d$.

$\psi = \left(\frac{\mu_c}{\mu_d}\ \phi_d^{2.5} + \frac{\mu_d}{\mu_c}\ \phi_c^{2.5}\right)^{-0.70}$, viscosity-volume-fraction parameter used in the coalescence correlation.

LITERATURE CITED

1. Batchelor, G. F., Proc. Cambridge Phil. Soc., 47, 359 (1951).
2. Calderbank, P. H., Brit. Chem. Eng. 1, 206 (1956).
3. Clay, P. C., Proc. Acad. Sci. Amsterdam, 43, 832, 979 (1940).
4. Fick, J. L., H. E. Rea, and T. Vermeulen, "The Effects of Agitator Geometry in the Mixing of Liquid-liquid Systems," UCRL-2545, April, 1954.
5. Hinze, J. O., A. I. Ch. E. Journal 1, 289 (1955).
6. Hulst, H. C. van de, Light Scattering by Small Particles, (John Wiley, New York, 1957).
7. Laity, D. S. and R. E. Treybal, A. I. Ch. E. Journal 3, 176 (1957).
8. Langlois, G. E., J. E. Gullberg, and T. Vermeulen, Rev. Sci. Insts. 25, 360 (1954).
9. Rodger, W. A., V. G. Trice, Jr., and J. H. Rushton, Chem. Eng. Progress 52, 515 (1956).
10. Rushton, J. H., E. W. Costich, and H. J. Everett, Chem. Eng. Prog. 46, 395 (1950).
11. Shinnar, R., and Church, J. M., Ind. Eng. Chem. 52, 253 (1960).
12. Trice, V. G., Jr., and W. A. Rodger, A. I. Ch. E. Journal 2, 205 (1956).
13. Vand, V., J. Phys. and Colloid Chem. 52, 277 (1948).
14. Vermeulen, T., G. M. Williams, and G. E. Langlois, Chem. Eng. Prog. 51, 85 (1955).
15. Webster, D. S., paper presented at A. I. Ch. E. 39th National Meeting, Atlantic City, N. J. (March 1959).

APPENDIX

I. Numerical Data

Table IV. Drop Size Profile for Liquid-Liquid Systems

ϕ	N RPS	d_0, cm. (calc.)	Diameter (cm.) at Locations A	B	C	D	E
			Butanol in Water				
0.10	2.57	0.00453	0.01052		0.01104	0.01190	0.01284
	4.12	0.00257	0.00528		0.00582	0.00658	0.00690
	6.45	0.00150	0.00281		0.00314	0.00374	0.00411
0.40	2.57	0.00725	0.01680		0.01943	0.02240	0.02421
	4.12	0.00411	0.00832		0.00989	0.01259	0.01331
	6.45	0.00240	0.00509		0.00588	0.00706	0.00779
			Water in Butanol				
0.10	2.57	0.00444	0.01393	0.01444	0.01546	0.01717	0.01755
	4.12	0.00252	0.00803	0.00834	0.00948	0.01141	0.01174
	6.45	0.00147	0.00450	0.00477	0.00566	0.00725	0.00772
	2.57	0.00444	0.01500		0.01630	0.01731	0.01741
	4.12	0.00252	0.00845		0.00952	0.01102	0.01131
	6.45	0.00147	0.00490		0.00560	0.00701	0.00728
0.40	2.57	0.00711	0.01283		0.01504	0.01789	0.01975
	4.12	0.00403	0.00664		0.00796	0.01011	0.01098
	6.45	0.00236	0.00423		0.00482	0.00615	0.00650
	2.57	0.00711	0.01399	0.01373	0.01548	0.01761	0.01865
	4.12	0.00403	0.00699	0.00711	0.00806	0.00998	0.01051
	6.45	0.00236	0.00438	0.00449	0.00496	0.00592	0.00649
			Methyl Isobutyl Ketone in Water				
0.10	2.57	0.01285	0.04361		0.04955	0.05441	0.05345
	4.12	0.00728	0.02357		0.02860	0.03453	0.03508
	6.45	0.00426	0.01249		0.01609	0.02112	0.02339
	4.12	0.00728	0.02612		0.03035	0.03348	0.03413
	6.45	0.00426	0.01443		0.01806	0.02303	0.02478
0.40	2.57	0.02050	0.07993		0.09583	0.12982	0.14000
	4.12	0.01164	0.04036		0.05418	0.07267	0.07850
	6.45	0.00680	0.02083		0.02963	0.04398	0.04735
			Water in Methyl Isobutyl Ketone				
0.10	4.12	0.00709	0.01314	0.01376	0.01394	0.01480	0.01496
	6.45	0.00414	0.00733	0.00826	0.00843	0.00965	0.00989
0.40	2.57	0.02191	0.03232		0.03329	0.03429	0.03550
	4.12	0.01244	0.02000		0.02132	0.02279	0.02330
	6.45	0.00725	0.01229		0.01359	0.01547	0.01600
			Cyclohexanone in Water				
0.10	2.57	0.00662	0.01610	0.01696	0.01774	0.01968	0.01980
	4.12	0.00376	0.00777	0.00820	0.00911	0.01084	0.01107
	6.45	0.00220	0.00384	0.00407	0.00463	0.00590	0.00633
0.40	2.57	0.01060	0.02389	0.02817	0.00320	0.03374	0.04155
	4.12	0.00602	0.01247	0.01515	0.01719	0.01903	0.02290
	6.45	0.00352	0.00779	0.00947	0.01003	0.01176	0.01410
			Water in Cyclohexanone				
0.10	2.57	0.00654	0.00932	0.00955	0.01018	0.01115	0.01182
	4.12	0.00371	0.00529	0.00544	0.00585	0.00676	0.00712
	6.45	0.00217	0.00324	0.00337	0.00362	0.00432	0.00455
0.40	2.57	0.01046	0.01650	0.01648	0.01761	0.01991	0.02107
	4.12	0.00594	0.01039	0.01041	0.01129	0.01323	0.01375
	6.45	0.00347	0.00724	0.00734	0.00808	0.00934	0.00975
			Di-isobutyl Carbinol in Water				
0.10	6.45	0.00526	0.00546	0.00566	0.00566	0.00579	0.00585
0.40	6.45	0.00919	0.01138	0.01156	0.01177	0.01214	0.01224
			Water in Di-isobutyl Carbinol				
0.10	6.45	0.00559	0.02052	0.02361	0.02900	0.03147	0.03510
0.40	4.12	0.01529	0.01336	0.01350	0.01391	0.01408	0.01494
	6.45	0.00895	0.00876	0.00890	0.00917	0.00930	0.00950
			Glycol in Methyl Isobutyl Ketone				
0.10	6.45	0.00210	0.00405	0.00411	0.00435	0.00461	0.00461
0.40	4.12	0.00535	0.01193	0.01235	0.01315	0.01399	0.01426
	6.45	0.00313	0.00689	0.00705	0.00754	0.00809	0.00816
			Methyl Isobutyl Ketone in Glycol				
0.10	6.45	0.00201	0.01093	0.01169	0.01348	0.01634	0.01746
0.40	4.12	0.00549	0.00972	0.01016	0.01072	0.01172	0.01206
	6.45	0.00322	0.00595	0.00617	0.00652	0.00709	0.00720
			Experiments with Double-Width (2.0-inch) Impeller				
			Methyl Isobutyl Ketone in Water				
0.40	2.57	0.02055	0.05379	0.05630	0.06111	0.06981	0.06981
	4.12	0.01164	0.02960	0.03222	0.03787	0.04512	0.04512
	6.45	0.00680	0.01590	0.01758	0.02130	0.02708	0.02708
			Water in Isobutyl Ketone				
0.40	4.12	0.01244	0.01498	0.01538	0.01601	0.01673	0.01673
	6.45	0.00725	0.00919	0.00952	0.01007	0.01074	0.01086
			Methyl Isobutyl Ketone in Glycol				
0.10	6.45	0.00201	0.01092	0.01137	0.01261	0.01504	0.01538
0.40	4.12	0.00549	0.00847	0.00871	0.00910	0.00951	0.00951
	6.45	0.00322	0.00558	0.00569	0.00585	0.00607	0.00610
			Glycol in Methyl Isobutyl Ketone				
0.40	6.45	0.00313	0.00601	0.00674	0.00712	0.00742	0.00742

Table V. Predicted Versus Observed Drop Diameters

ϕ	N	N_{We}	N_{Re}	ψ	d_A obs.	d_A calc.	d_D obs.	d_D calc.
				Butanol in Water				
0.10	2.57	6900	31500	1.066	0.01052	0.00778	0.01190	0.00968
	4.12	17800	50400	0.881	0.00528	0.00525	0.00658	0.00683
	6.45	43500	79000	0.738	0.00281	0.00375	0.00374	0.00507
0.40	2.57	6900	31500	3.165	0.01677	0.01691	0.02240	0.02255
	4.12	17800	50400	2.618	0.00832	0.01210	0.01259	0.01675
	6.45	43500	79000	2.191	0.00509	0.00909	0.00706	0.01299
				Water in Butanol				
0.10	2.57	5960	10540	2.244	0.01393	0.01130	0.01717	0.01526
	4.12	15350	16860	1.856	0.00803	0.00818	0.01141	0.01148
	6.45	37600	26400	1.553	0.00450	0.00622	0.00725	0.00897
	2.57	5960	10654	2.244	0.01500	0.01130	0.01731	0.01526
	4.12	15350	16860	1.856	0.00845	0.00818	0.01102	0.01148
	6.45	37600	26400	1.553	0.00490	0.00622	0.00701	0.00897
0.40	2.57	5960	10540	2.984	0.01283	0.01621	0.01789	0.02152
	4.12	15350	16860	2.468	0.00664	0.01155	0.01011	0.01595
	6.45	37600	26400	2.066	0.00423	0.00866	0.00615	0.01234
	2.57	5960	10540	2.984	0.01399	0.01621	0.01761	0.02152
	4.12	15350	16860	2.468	0.00699	0.01155	0.00998	0.01595
	6.45	37600	26400	2.066	0.00438	0.00866	0.00592	0.01234
				Methyl Isobutyl Ketone in Water				
0.10	2.57	1280	41200	6.637	0.04361	0.03310	0.05441	0.04491
	4.12	3300	66200	5.490	0.02357	0.02405	0.03453	0.03382
	6.45	8080	103500	4.590	0.01249	0.01825	0.02112	0.02641
	4.12	3300	66200	5.490	0.02612	0.02405	0.03348	0.03382
	6.45	8080	103500	4.590	0.01443	0.01825	0.02303	0.02641
0.40	2.57	1280	41200	12.509	0.07993	0.05870	0.12982	0.08100
	4.12	3300	66200	10.347	0.04036	0.04320	0.07267	0.06160
	6.45	8080	103500	8.650	0.02083	0.03315	0.04398	0.04860
				Water in Methyl Isobutly Ketone				
0.10	4.12	2640	89600	3.775	0.01314	0.01860	0.01480	0.02532
	6.45	6460	140000	3.155	0.00733	0.01375	0.00965	0.01938
0.40	2.57	1025	55800	13.650	0.03232			
	4.12	2640	89600	11.200	0.02000	0.04660	0.02279	0.06640
	6.45	6460	140000	9.310	0.01229	0.03560	0.01547	0.05220
				Cyclohexanone in Water				
0.10	2.57	3510	31700	1.851	0.01610	0.01228	0.01968	0.01556
	4.12	9050	50800	1.533	0.00777	0.00844	0.01084	0.01117
	6.45	22150	79500	1.283	0.00384	0.00611	0.00590	0.00840
0.40	2.57	3510	31700	5.287	0.02389	0.02620	0.03374	0.03615
	4.12	9050	50800	4.378	0.01247	0.01935	0.01903	0.02718
	6.45	22150	79500	3.665	0.00779	0.01469	0.01176	0.02122
				Water in Cyclohexanone				
0.10	2.57	3350	17080	2.966	0.00932	0.01559	0.01115	0.02089
	4.12	8620	27400	2.455	0.00529	0.01120	0.00676	0.01560
	6.45	21100	42850	2.054	0.00324	0.00843	0.00432	0.01209
0.40	2.57	3350	17080	5.426	0.01650	0.02700	0.01991	0.03671
	4.12	8620	27400	4.491	0.01039	0.01964	0.01323	0.02762
	6.45	21100	42850	3.757	0.00724	0.01494	0.00934	0.02163
				Di-isobutyl Carbinol in Water				
0.10	6.45	4920	103600	0.852	0.00546	0.00771	0.00579	
0.40	6.45	4920	103600	2.747	0.01138	0.01758	0.01214	
				Water in Di-isobutyl Carbinol				
0.10	6.45	3960	8330	4.914	0.02052	0.02059	0.03147	
0.40	4.12	1615	5320	1.826	0.01336	0.02090	0.01408	0.02415
	6.45	3960	8330	1.526	0.00876	0.01361	0.00930	0.01634
				Glycol in Methyl Isobutyl Ketone				
0.10	6.45	22900	128700	0.263	0.00405	0.00290	0.00461	
0.40	4.12	9350	82200	0.905	0.01193	0.00812	0.01399	0.00972
	6.45	22900	128700	0.756	0.00689	0.00544	0.00809	0.00676
				Methyl Isobutyl Ketone in Glycol				
0.10	6.45	30200	7290	2.150	0.01093	0.00856	0.01634	0.01238
0.40	4.12	12350	4650	0.444	0.00972	0.00685	0.01172	0.00764
	6.45	30200	7290	0.371	0.00595	0.00435	0.00709	0.00502
				Experiments with Double-width Impeller				
				Methyl Isobutyl Ketone in Water				
0.40	2.57	1280	41200	12.509	0.05379	0.05870	0.06981	0.08100
	4.12	3300	66200	10.347	0.02960	0.04320	0.04512	0.06160
	6.45	8080	103500	650	0.01594	0.03315	0.02708	0.04860
				Water in Methyl Isobutyl Ketone				
0.40	4.12	2640	89600	11.200	0.01498	0.04660	0.01673	0.06640
	6.45	6460	140000	9.310	0.00919	0.04560	0.01074	0.05520
				Methyl Isobutyl Ketone in Glycol				
0.10	6.45	30200	7290	2.150	0.01092	0.00856	0.01504	0.01238
0.40	4.12	12350	4650	0.444	0.00847	0.00685	0.00951	0.00764
	6.45	30200	7290	0.371	0.00558	0.00435	0.00607	0.00502
				Glycol in Methyl Isobutyl Ketone				
0.40	22900		128700	0.756	0.00601	0.00544	0.00742	0.00676

Table VI. Predicted vs Observed Drop Diameters for Langlois' Data (L = 17.2 cm)

ϕ	N	N_{We}	N_{Re} $\times 10^{-4}$	ψ	d_0 (Eq. 9)	d_{obs}	d_{calc}
				Water in Isooctane			
0.20	2.00	384	7.48	13.22	0.0398	0.0980	0.0492
	2.52	611	9.41	12.04	0.0302	0.0747	0.0386
	3.15	952	12.2	11.03	0.0231	0.0506	0.0308
	4.26	1750	16.0	9.75	0.0161	0.0345	0.0228
	4.50	1950	16.7	9.54	0.0150	0.0315	0.0217
	5.34	2740	20.0	8.92	0.0123	0.0248	0.0185
	6.67	4270	25.3	8.17	0.0094	0.0182	0.0151
				Water in Kerosene			
0.10	1.85	495	2.24	8.74	0.0285	0.0615	0.0347
	2.33	781	2.82	7.99	0.0218	0.0412	0.0273
	3.17	1440	3.84	7.07	0.0150	0.0230	0.0200
	4.10	2420	4.96	6.37	0.0110	0.0146	0.0155
	5.00	3600	6.05	5.88	0.0087	0.0106	0.0128
	6.67	6400	8.08	5.24	0.0061	0.0087	0.0098
0.20	1.83	482	2.21	12.55	0.0348	0.0624	0.0436
	2.37	810	2.87	11.30	0.0255	0.0441	0.0334
	3.25	1530	3.93	9.94	0.0174	0.0272	0.0244
	3.93	2240	4.76	9.21	0.0139	0.0197	0.0203
	5.00	3600	6.05	8.39	0.0104	0.0154	0.0164
	6.67	6400	8.08	7.48	0.0074	0.0117	0.0126
0.40	1.83	482	2.21	15.80	0.0465	0.0695	0.0576
	2.37	810	2.87	14.24	0.0340	0.0442	0.0440
	3.12	1410	3.78	12.73	0.0244	0.0314	0.0333
	3.85	2130	4.66	11.75	0.0191	0.0265	0.0273
	4.00	2300	4.84	11.57	0.0181	0.0242	0.0263
	4.97	3560	6.01	10.59	0.0140	0.0212	0.0214
	6.67	2400	8.08	9.42	0.0098	0.0177	0.0165
				Water in Blend A (White oil plus kerosene, vis. 65.4 cp.)			
0.20	1.87	332	0.068	1.06	0.0439	0.0522	0.0446
	2.61	648	0.095	0.93	0.0293	0.0292	0.0300
	3.42	1110	0.125	0.83	0.0202	0.0187	0.0218
	3.66	1270	0.134	0.81	0.0196	0.0182	0.0202
	4.77	2160	0.174	0.73	0.0142	0.0132	0.0148
	6.67	4210	0.214	0.64	0.0096	0.0108	0.0100
				Water in Blend B (White oil plus kerosene, vis. 15.6 cp.)			
0.20	1.70	280	0.255	5.62	0.0485	0.0670	0.0524
	2.02	393	0.303	5.26	0.0395	0.0412	0.0432
	2.32	520	0.348	4.97	0.0334	0.0328	0.0369
	4.67	2110	0.700	3.75	0.0144	0.0150	0.0171
	6.67	4300	1.000	3.25	0.0094	0.0111	0.0117
0.40	1.82	319	0.316	2.22	0.0594	0.0870	0.0610
	2.42	566	0.420	1.98	0.0421	0.0515	0.0435
	3.17	963	0.550	1.78	0.0306	0.0383	0.0319
	4.50	1940	0.780	1.55	0.0201	0.0294	0.0212
	6.67	4300	1.175	1.32	0.0125	0.0203	0.0134
				Water in White Oil			
0.20	1.89	315	0.0249	0.34	0.0453	0.0560	0.0455
	2.67	625	0.0353	0.30	0.0300	0.0375	0.0302
	4.00	1400	0.0529	0.25	0.0185	0.0252	0.0187
	6.67	3900	0.0881	0.21	0.0100	0.0186	0.0101
				White Oil in Water			
0.20	1.90	308	5.31	0.40	0.0457	0.0658	0.0460
	2.46	515	6.86	0.36	0.0336	0.0386	0.0339
	3.17	852	8.85	0.33	0.0255	0.0267	0.0258
	4.04	1390	11.29	0.30	0.0185	0.0206	0.0187
	5.24	2340	14.65	0.27	0.0135	0.0158	0.0137
	6.67	3790	18.65	0.24	0.0101	0.0121	0.0103
				Water in Blend C (CCl_4 plus isooctane, density 1.033 gm/cm^3)			
0.10	1.85	413	8.2	8.73	0.0318	0.0583	0.0379
	2.54	776	11.2	7.71	0.0218	0.0314	0.0272
	3.16	1200	13.9	7.06	0.0168	0.0210	0.0217
	4.58	2530	20.2	6.08	0.0107	0.0133	0.0150
	6.67	5350	29.4	5.24	0.0069	0.0084	0.0105
0.20	1.79	386	7.9	13.39	0.0399	0.0780	0.0493
	2.05	505	9.2	12.70	0.0340	0.0595	0.0429
	2.43	710	10.7	11.86	0.0277	0.0446	0.0361
	2.72	890	12.0	11.33	0.0242	0.0382	0.0321
	3.03	1110	13.3	10.83	0.0212	0.0295	0.0288
	3.76	1710	16.5	9.93	0.0163	0.0227	0.0233
	4.16	2100	18.3	9.52	0.0144	0.0169	0.0211
	4.83	2825	21.2	8.99	0.0121	0.0161	0.0184
	6.67	5350	29.4	7.92	0.0082	0.0104	0.0138
0.40	1.87	421	8.35	24.37	0.0504	0.1145	0.0675
	2.65	895	11.8	21.21	0.0332	0.0580	0.0481
	3.58	15.40	15.9	18.81	0.0231	0.0330	0.0363
	5.43	3550	24.2	15.91	0.0140	0.0219	0.0252
	6.67	5350	29.8	14.66	0.0110	0.0167	0.0212
				Carbon Disulfide in Water			
0.20	1.67	470	4.67	21.86	0.0354	0.0450	0.0507
	2.44	1000	6.82	18.81	0.0225	0.0215	0.0357
	3.38	2030	10.00	16.10	0.0147	0.0158	0.0260
	4.70	3700	13.2	14.49	0.0102	0.0133	0.0204
	6.67	7400	18.7	12.64	0.0068	0.0116	0.0156
0.40	1.74	510	4.80	20.64	0.0451	0.0490	0.0596
	2.40	970	6.62	18.15	0.0307	0.0298	0.0434
	3.27	1800	9.04	16.04	0.0212	0.0241	0.0324
	4.77	3820	13.2	13.81	0.0135	0.0198	0.0232
	6.67	7400	18.4	12.13	0.0091	0.0165	0.0176
				Water in Carbon Disulfide			
0.20	2.07	688	19.1	11.17	0.0283	0.0312	0.0362
	2.30	850	23.0	10.71	0.0250	0.0258	0.0325
	3.18	1620	29.3	9.42	0.0169	0.0213	0.0235
	3.50	1980	32.2	9.03	0.0150	0.0190	0.0213
	5.00	4010	46.0	7.85	0.0098	0.0175	0.0154
	6.67	7050	61.5	7.04	0.0070	0.0147	0.0119
				Isooctane in Water			
0.10	2.50	558	7.0	14.59	0.0257	0.0217	0.0360
	3.40	1030	9.5	13.22	0.0184	0.0162	0.0272
	4.70	1960	13.1	11.63	0.0125	0.0121	0.0207
	6.67	3970	18.6	10.09	0.0082	0.0092	0.0152
0.20	1.83	299	5.1	23.95	0.0463	0.0502	0.0632
	2.40	515	6.7	21.47	0.0335	0.0276	0.0485
	3.30	975	9.2	18.89	0.0228	0.0195	0.0361
	4.70	1960	13.1	16.47	0.0150	0.0148	0.0265
	6.67	3970	18.6	14.28	0.0098	0.0116	0.0198
0.40	1.70	259	4.8	29.73	0.0674	0.0743	0.0883
	2.35	493	6.6	26.16	0.0458	0.0381	0.0642
	4.10	1500	11.5	20.94	0.0235	0.0241	0.0382
	6.67	3970	18.6	17.24	0.0131	0.0173	0.0250

II. Photoelectric-Probe Calibration Curves

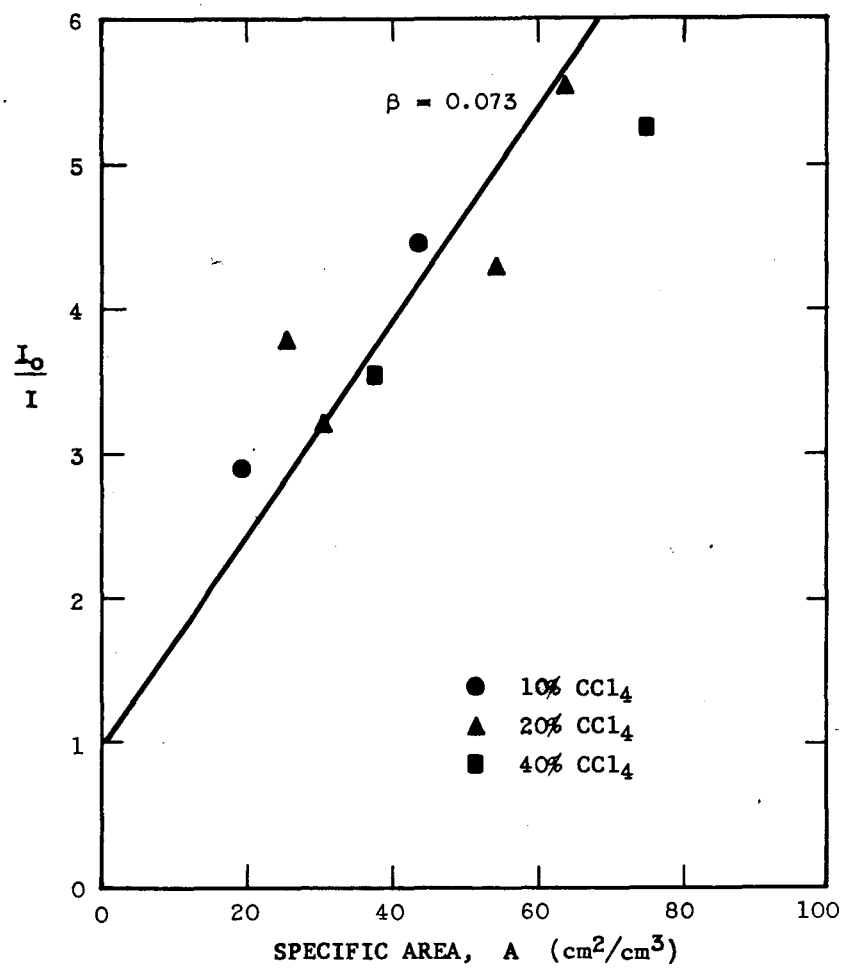

MU-17572

Fig. 20. Photocell calibration curve -- CCl_4 in water.

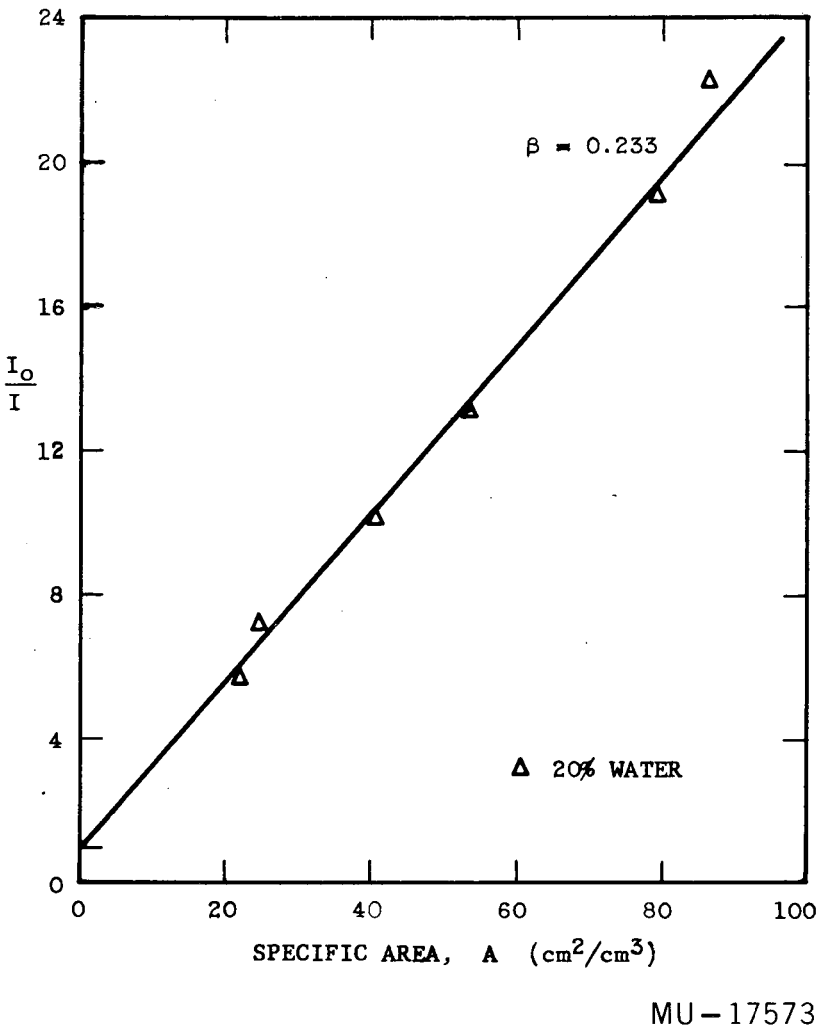

Fig. 21. Photocell calibration curve -- water in CS_2.

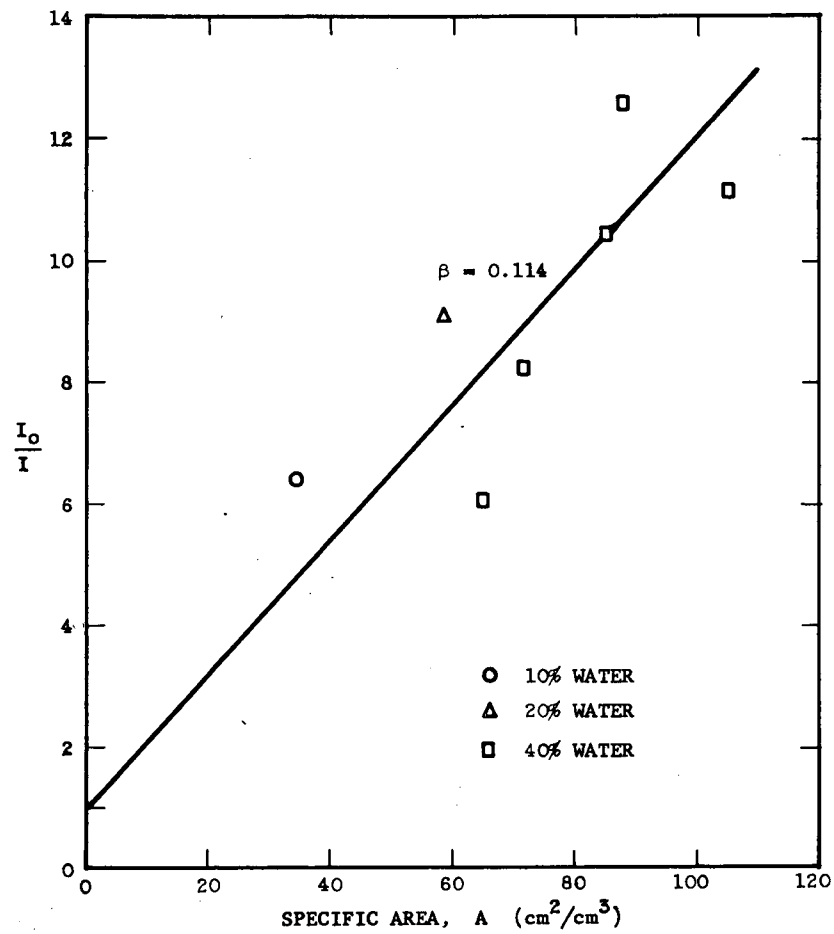

MU-17574

Fig. 22. Photocell calibration curve -- water in CCl_4.

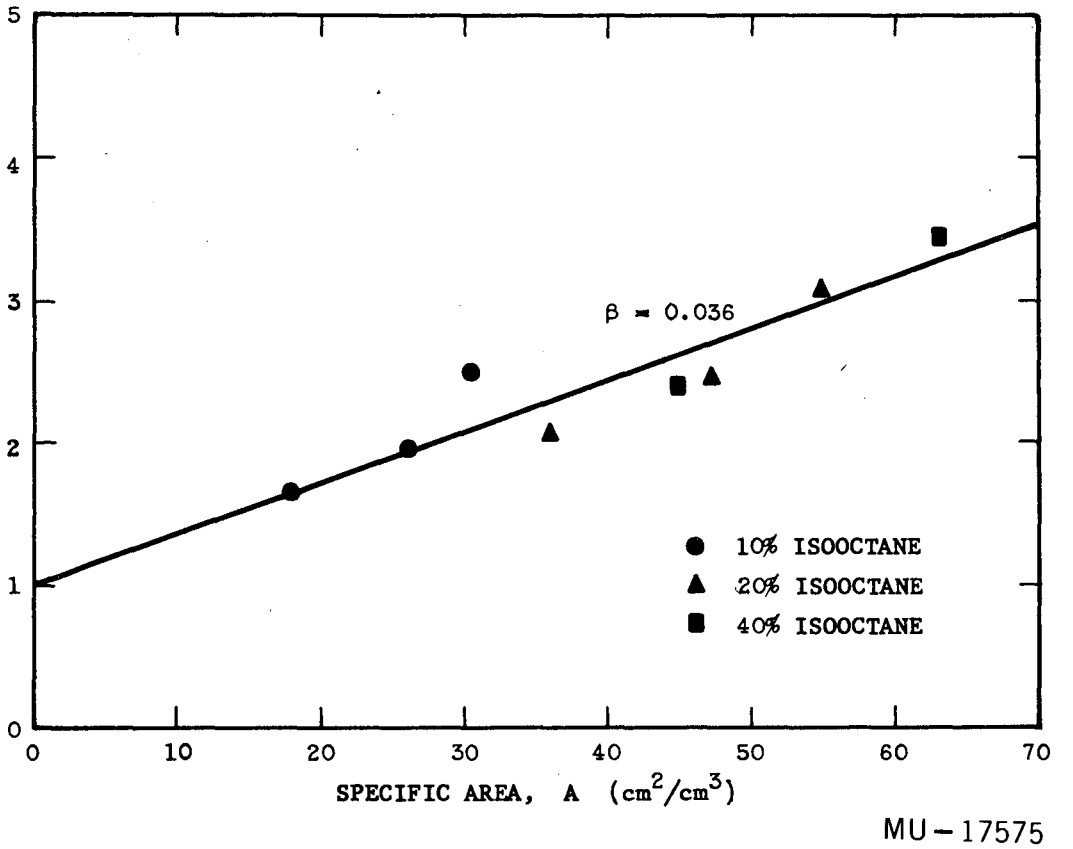

Fig. 23. Photocell calibration curve -- isooctane in water.

This report was prepared as an account of Government sponsored work. Neither the United States, nor the Commission, nor any person acting on behalf of the Commission:

A. Makes any warranty or representation, expressed or implied, with respect to the accuracy, completeness, or usefulness of the information contained in this report, or that the use of any information, apparatus, method, or process disclosed in this report may not infringe privately owned rights; or

B. Assumes any liabilities with respect to the use of, or for damages resulting from the use of any information, apparatus, method, or process disclosed in this report.

As used in the above, "person acting on behalf of the Commission" includes any employee or contractor of the Commission, or employee of such contractor, to the extent that such employee or contractor of the Commission, or employee of such contractor prepares, disseminates, or provides access to, any information pursuant to his employment or contract with the Commission, or his employment with such contractor.